

SELECTED HYDRAULIC TEST ANALYSIS TECHNIQUES
FOR CONSTANT-RATE DISCHARGE TESTS

F. A. Spane, Jr.

March 1993

Prepared for
the U.S. Department of Energy
under Contract DE-AC06-76RLO 1830

Pacific Northwest Laboratory
Richland, Washington 99352

MASTER

ds
DISTRIBUTION OF THIS DOCUMENT IS UNLIMITED

SUMMARY

The constant-rate discharge test is the principal field method used in hydrogeologic investigations for characterizing the hydraulic properties of aquifers. To implement this test, the aquifer is stressed by withdrawing ground water from a well, by using a downhole pump. Discharge during the withdrawal period is regulated and maintained at a constant rate. Water-level response within the well is monitored during the active pumping phase (i.e., drawdown) and during the subsequent recovery phase following termination of pumping. The analysis of drawdown and recovery response within the stress well (and any monitored, nearby observation wells) provides a means for estimating the hydraulic properties of the tested aquifer, as well as discerning formational and nonformational flow conditions (e.g., wellbore storage, wellbore damage, presence of boundaries, etc.). Standard analytical methods that are used for constant-rate pumping tests include both log-log type-curve matching and semi-log straight-line methods.

This report presents a current "state of the art" review of selected transient analysis procedures for constant-rate discharge tests. Specific topics examined include: analytical methods for constant-rate discharge tests conducted within confined and unconfined aquifers; effects of various non-ideal formation factors (e.g., anisotropy, hydrologic boundaries) and well construction conditions (e.g., partial penetration, wellbore storage) on constant-rate test response; and the use of pressure derivatives in diagnostic analysis for the identification of specific formation, well construction, and boundary conditions.

Of particular note is the contribution that pressure derivative analysis provides in removing test analysis ambiguity. When used in combination with standard log-log pressure change versus time plots, pressure derivatives can be used to identify specific test formation behavior and to significantly improve log-log type curve match analysis.

Information presented in this report can be used for the proper design and analysis of constant-rate discharge tests conducted in support of hydrologic characterization investigations on the Hanford Site, for a variety of

formation and test conditions. Although the discussion pertains mainly to tests conducted within granular sedimentary aquifers, the information is also applicable to fractured aquifer systems that can be characterized as porous media equivalents.

ACKNOWLEDGMENTS

A number of people provided contributions in the development of this report. In particular, important technical peer review contributions were provided by P. D. Thorne and T. J Gilmore. In addition, the editorial review and guidance provided by R. E. Schrempf and J. B. Flynn are also acknowledged.

CONTENTS

SUMMARY	iii
ACKNOWLEDGMENTS	v
1.0 INTRODUCTION	1.1
2.0 PRESSURE DERIVATIVE ANALYSIS	2.1
3.0 CONSTANT-RATE DISCHARGE TEST SOLUTIONS/ANALYSES	3.1
3.1 NONLEAKY CONFINED AQUIFERS	3.1
3.1.1 Pressure Derivative Applications	3.7
3.1.2 Analysis Guidelines	3.9
3.2 LEAKY CONFINED AQUIFERS	3.13
3.2.1 Leaky Conditions with Confining Layer Storage	3.13
3.2.2 Leaky Conditions Without Confining Layer Storage	3.15
3.2.3 Analysis Guidelines	3.18
3.3 UNCONFINED AQUIFERS	3.20
3.3.1 Unconfined Aquifer - Type Curve Analysis	3.20
3.3.2 Confined Aquifer Solution Analysis	3.26
4.0 FACTORS AFFECTING HYDRAULIC TEST ANALYSIS	4.1
4.1 WELL CONSTRUCTION CONDITIONS	4.1
4.1.1 Wellbore Storage	4.1
4.1.2 Wellbore Damage	4.4
4.1.3 Partial Penetration	4.6
4.2 FORMATION CONDITIONS	4.11
4.2.1 Anisotropy	4.11
4.2.2 Hydrologic Boundaries	4.12
4.3 EXTERNAL STRESS FACTORS	4.15

4.3.1	Barometric Fluctuation	4.16
4.3.2	River-Stage Fluctuation	4.18
4.3.3	Extraneous Stress Removal	4.19
5.0	TEST DATA ANALYSIS	5.1
5.1	CONFINED AQUIFER EXAMPLES	5.1
5.1.1	Nonleaky Test Example	5.1
5.1.2	Leaky Test Example	5.3
5.2	UNCONFINED AQUIFER EXAMPLE	5.6
5.2.1	Analysis Using the Confined Aquifer Solution	5.6
5.2.2	Unconfined Aquifer - Type-Curve Analysis	5.8
6.0	REFERENCES	6.1

FIGURES

3.1	Exact Solution for Nonleaky Confined Aquifers, for Various Dimensionless Distance Relationships	3.4
3.2	Error Induced by Using the Theis Solution for Various Dimensionless Distances	3.5
3.3	Dimensionless Pressure and Dimensionless Pressure Derivative Type Curves for Constant-Rate Pumping Tests	3.8
3.4	Characteristic Log-Log Pressure and Pressure Derivative Plots for Various Hydrogeologic Formation/Boundary Conditions	3.10
3.5	Dimensionless Drawdown Type Curves for Constant-Rate Discharge Tests in Leaky Confined Aquifers With Confining Layer Storage	3.15
3.6	Dimensionless Drawdown Derivative Type Curves for Constant-Rate Discharge Tests in Leaky Confined Aquifers With Confining Layer Storage	3.16
3.7	Dimensionless Drawdown and Dimensionless Drawdown Derivative Type Curves for Constant-Rate Discharge Tests in Leaky Confined Aquifers Without Confining Layer Storage	3.17
3.8	Dimensionless Time-Drawdown Type Curves for Constant-Rate Discharge Tests in Unconfined Aquifers for $\sigma = 10^{-3}$	3.22
3.9	Dimensionless Drawdown Type Curves for Constant-Rate Discharge Tests Unconfined Aquifer Delayed-Yield Type A Curves	3.23
3.10	Dimensionless Drawdown Type Curves for Constant-Rate Discharge Tests Unconfined Aquifer Delayed-Yield Type B Curves	3.23
3.11	Dimensionless Drawdown Derivative Type Curves for Constant-Rate Discharge Tests Unconfined Aquifer Delayed-Yield Type A Curves	3.24
3.12	Dimensionless Drawdown Derivative Type Curves for Constant-Rate Discharge Tests Unconfined Aquifer Delayed-Yield Type B Curves	3.24
4.1	Effects of Wellbore Storage During Constant-Rate Discharge Tests for Selected Radial Distances	4.3

4.2	Dimensionless Pressure and Dimensionless Pressure Derivative Type Curves for Constant-Rate Pumping Tests	4.5
4.3	Effects of a Partially Penetrating Pumping Well Completed in the Lower 30% of a Confined Aquifer	4.6
4.4	Partial Penetration Corrections for Selected Piezometer Depths Given a Pumping Well Screened Interval Depth, $z/b = 0.6$ to 0.9	4.8
4.5	Characteristic Unconfined Aquifer Behavior During Constant-Rate Discharge Tests for $K_0 = 1.0$ $r = b$	4.9
4.6	Effects of Partial Penetration Within an Unconfined Aquifer During Constant-Rate Testing	4.10
4.7	Effect of an Impermeable Boundary During Constant-Rate Testing for Dimensionless Distances of $r_0 = 750$ and 7500	4.14
4.8	Example of External Stress Factor Removal for Well DB-2: (a) Comparison of Uncorrected DB-2 Water Levels and Columbia River-Stage Fluctuations and (b) Comparison of River-Stage Corrected DB-2 Water Levels and Atmospheric Pressure Variations	4.20
4.9	Comparison of Uncorrected Well DB-2 Water Levels and Fully Corrected Well DB-2 Water Levels with Extraneous Stress Effects Removed	4.21
5.1	Diagnostic Log-Log Analysis Plot and Type Curve Match for Nonleaky Confined Aquifer Test Example	5.2
5.2	Semi-Log, Straight-Line Analysis for Nonleaky Confined Aquifer Test Example	5.3
5.3	Diagnostic Log-Log Analysis Plot and Type Curve Match for Leaky Confined Aquifer Test Example	5.5
5.4	Diagnostic Log-Log Analysis Plot for Unconfined Aquifer Test Example	5.8
5.5	Semi-Log, Straight-Line Analysis for Unconfined Aquifer Test Example	5.9
5.6	Confined Aquifer Type Curve Analysis for Unconfined Aquifer Test Example	5.10
5.7	Unconfined Aquifer Type A Curve and Derivative Analysis for Unconfined Aquifer Test Example	5.11

5.8	Unconfined Aquifer Type B Curve and Derivative Analysis for Unconfined Aquifer Test Example	5.12
5.9	Complete Unconfined Aquifer Type Curve Analysis for Unconfined Aquifer Test Example	5.13

1.0 INTRODUCTION

As part of the U.S. Department of Energy (DOE) Ground-Water Surveillance Project, Hanford Site Flow System Characterization Task, Pacific Northwest Laboratory (PNL) investigates the hydrogeologic properties that control the movement of contaminants within various aquifer systems on the Hanford Site, and assesses the potential for their migration offsite. As part of this activity, hydraulic property estimates, obtained from hydrogeologic characterization tests conducted at specific well locations on the Hanford Site, are routinely reported (e.g., Spane 1992a, 1992b; Thorne and Newcomer 1992).

In situ hydraulic properties of subsurface units are commonly determined using inverse analytical techniques that relate test response (i.e., the change of pressure with time) for a known imposed stress, to formation hydraulic properties (i.e., transmissivity and storativity). The principal method used in hydraulic characterization investigations is the constant-rate discharge test (i.e., a test where ground water is removed from a test interval at a constant rate for an extended period of time). Analysis of the change of pressure during the active or discharge phase (constant-rate discharge/drawdown analysis) and the subsequent recovery phase following termination of ground-water removal (constant-rate recovery analysis) are normally accomplished by type-curve fitting of log-log plots or straight-line analysis of semilogarithmic data plots of pressure change versus time. These analysis methods normally depend on assumed formation/test conditions such as: a homogeneous, isotropic aquifer of infinite lateral extent; fully penetrating/communicative wells possessing infinitesimally small borehole volumes; and radial flow conditions. Because of these constraining assumptions, it is important that the test analyst be familiar with the possible effects on test response, when these conditions and assumptions are not met.

Recent developments in diagnostic analysis using pressure derivatives has greatly facilitated the identification of nonformational and non-radial flow conditions within data obtained from constant-rate discharge tests. Recent computer program development has also provided the ability to design and analyze hydrologic tests for a variety of formation and test conditions.

The general objective of this report is to present a current "state of the art" review that can be used for the analysis and design of constant-rate discharge tests conducted in support of hydrologic characterization investigations on the Hanford Site. Specific report objectives include

- the review of analytical methods for constant-rate discharge tests conducted within confined and unconfined aquifers
- delineation of the effects that various heterogeneous formation factors (e.g., anisotropy, hydrologic boundaries) and well construction conditions (e.g., partial penetration, wellbore storage) have on constant-rate test response
- demonstration of the use of pressure derivatives in diagnostic analysis for identifying specific formation/flow/boundary conditions, and their use in hydraulic test analysis

Although this report pertains to constant-rate discharge tests conducted within largely granular sedimentary aquifer formations, the information is also applicable to analogous fracture aquifer systems that can be characterized as porous media equivalents.

2.0 PRESSURE DERIVATIVE ANALYSIS

Hydrologic test analysis based on the derivative of pressure (i.e., rate of pressure change) with respect to the natural logarithm of time has been shown to significantly improve the diagnostic and quantitative analysis of constant-rate discharge tests (i.e., pumping tests). The improvement in hydrologic test analysis is attributed to the sensitivity of the derivative response to small variations in the rate of pressure change that occurs during testing, which would otherwise be less obvious with standard pressure change versus time analysis techniques. The sensitivity of pressure derivatives to pressure change responses facilitates their use in identifying the presence of wellbore storage, boundaries, and establishment of radial flow conditions within the test data record.

One of the first papers to demonstrate the use of pressure derivatives to support the analysis of constant-rate discharge tests using the line-source solution was presented by Tiab and Kumar (1980). Following publication of this paper, many subsequent articles were published (e.g., Bourdet et al. 1983a, 1983b, 1984, 1989; Beauheim and Pickens 1986; Ehlig-Economides 1988, Mensch and Benson 1989, etc.), primarily in the petroleum industry, concerning the use of pressure derivative analysis for improving hydraulic test analysis and for discerning the flow response model that is operative during characterization of the test interval (i.e., homogeneous versus heterogeneous formation response). Recently, the use of pressure derivatives was also extended to the analysis of slug test response within confined aquifers (Karasaki et al. 1988; Ostrowski and Kloska 1989).

This vigorous response in the petroleum industry on the uses and application of pressure derivatives for hydraulic test analysis has not been matched within the hydrological sciences. One of the objectives of this report is to familiarize the reader with the use and application of pressure derivative analysis. A recent paper by Spane and Wurstner (1992) describes a computer program, DERIV, that can be used to convert hydrologic field test data obtained from slug and constant-rate discharge tests to pressure derivative format.

The following report sections include a description of the use of pressure derivatives for hydraulic test analysis of constant-rate discharge tests. In summary, pressure derivative analysis can improve constant-rate discharge test analysis over a wide range of aquifer/test conditions. Specifically, it can be used to

- diagnostically determine the appropriate formation response model (homogeneous versus heterogeneous) and boundary conditions (impermeable or constant head) that are evident during the test
- determine when infinite-acting, radial flow conditions are established and, therefore, when straight-line analysis of drawdown data is valid
- assist in log-log type-curve matching for test data exhibiting wellbore storage effects and boundary conditions

3.0 CONSTANT-RATE DISCHARGE TEST SOLUTIONS/ANALYSES

The constant-rate discharge test is the principal field method used in hydrogeologic investigations for the characterization of the hydraulic properties of aquifers. To implement this test, ground water is withdrawn from a well, commonly by using a downhole pump (e.g., submersible, turbine, etc.). Discharge during the withdrawal period is regulated and maintained at a constant rate. Water-level response within the well (and any monitored, nearby observation wells) is monitored during the active pumping phase (i.e., drawdown) and during the subsequent recovery phase following termination of pumping. The analysis of drawdown and recovery water-level response within the wells provides a means for estimating the hydraulic properties of the tested aquifer, and discerning formational and nonformational flow conditions (e.g., wellbore storage, wellbore damage, presence of boundaries, etc.).

Standard analytical methods that are used for constant-rate pumping tests include both log-log type-curve matching and semi-log straight-line methods. Since the initial transient analysis solution for constant-rate tests for fully penetrating wells within homogeneous, isotropic, confined aquifers was first published in Theis (1935), a multitude of papers have been published in ground-water and petroleum industry literature that provide transient solutions and analysis methods for constant-rate tests performed over a wide-range of formation and boundary conditions. Summaries of the development of these various solutions and analysis methods have appeared periodically (e.g., Weeks 1978; Witherspoon 1978; Ramey 1978, 1992). The historical development of constant-rate test analysis will not be presented in this report. The reader is directed to the cited references for a detailed discussion on this topic.

3.1 NONLEAKY CONFINED AQUIFERS

For confined aquifers, ground water produced during a constant-rate test is released by a number of mechanisms. For nonleaky confined aquifers, ground water is primarily released from elastic storage, including the expansion of

water and compression of the aquifer matrix. For leaky confined aquifers, ground water is also produced from elastic storage of the confining layers.

The solution for nonsteady ground-water flow to a well (line-source) within a nonleaky aquifer, which was developed from analogous heat flow equations, was first presented by Theis (1935). The Theis solution (also referred to as the exponential integral solution) relates drawdown within the aquifer to the transmissivity and storativity of the aquifer, for a given radial distance from a well pumped at a constant rate as follows:

$$s = \frac{Q}{4\pi T} \int_u^{\infty} (e^{-u}/u) du \quad (3.1)$$

where, the variable of integration, u , is defined by

$$u = r^2 S / 4 T t \quad (3.1a)$$

where s = drawdown [L]

T = transmissivity [L^2/T]

S = storativity [dimensionless]

Q = discharge rate [L^3/T]

r = radial distance from pumped well [L]

t = time since pumping started [T]

u = variable of integration [dimensionless].

The Theis solution is based on several assumptions concerning the aquifer and configuration of the pumped well. Weeks (1979) has grouped these assumptions into three categories:

1. Aquifer

- a) infinite in areal extent
- b) confined above and below by impermeable beds (i.e., nonleaky)
- c) homogeneous, isotropic, and of uniform thickness
- d) remains filled with water
- e) releases water from storage instantaneously with a decline in head

2. Pumped Well

- a) completely penetrates the aquifer
- b) infinitesimal well diameter
- c) produces water without head loss in the well bore
- d) uniform flow to the well per unit length open to the aquifer

3. Stress Application

- a) Stress (i.e., flow rate) applied at the pumped well is constant, starting at some initial time $t = 0$.

The effect on transient test response of not meeting some of the identified assumptions (i.e., 1a,b,c and 2a,b,c) is addressed in various subsections of this report.

As indicated in Lohman (1972), Equation (3.1) cannot be directly integrated, but its value is given by the infinite series presented in the following equation:

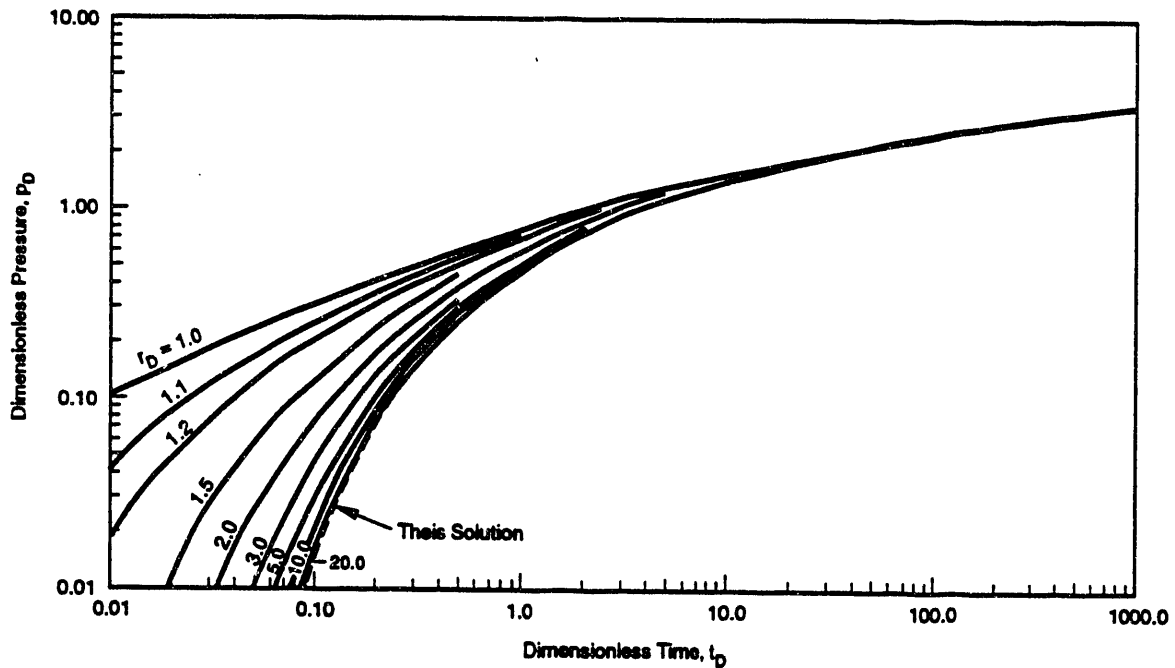
$$s = \frac{Q}{4\pi T} [-0.577216 - \ln u + u - (u^2/2 \cdot 2!) + (u^3/3 \cdot 3!) - \dots] \quad (3.2)$$

The value of the series relationship in Equation (3.2) is commonly expressed as $W(u)$ - the well function of u , for which tabulated values are presented in Ferris et al. (1962). Drawdown, using this relationship, is defined as:

$$s = \frac{Q W(u)}{4 \pi T} \quad (3.3)$$

Figure 3.1 shows the exact solution for nonsteady flow at various dimensionless radial distances from the pumping well, as presented in Mueller and Witherspoon (1965). Dimensionless parameters shown in the figure are defined below:

$$p_D = (2\pi T/Q)\Delta h \quad (3.4)$$



S9210002.12

FIGURE 3.1. Exact Solution for Nonleaky Confined Aquifers, for Various Dimensionless Distance Relationships (adapted from Mueller and Witherspoon 1965)

$$t_D = (T t)/(r^2 S) \quad (3.5)$$

$$r_D = r_o/r_w \quad (3.6)$$

where p_D = dimensionless pressure change

t_D = dimensionless time; equal to $1/(4 u)$

r_o = observation well distance from pumping well [L]

r_w = stress well radius in test interval [L].

As indicated in Figure 3.1, the Theis solution provides an accurate description of pressure change for all dimensionless times for dimensionless distances greater than 20.

Figure 3.2 shows the error induced by using the Theis solution for various dimensionless distances from the stress well. Mueller and Witherspoon (1965) state that after a dimensionless time of 50, the Theis solution can be used with an error of only 1 percent (or less) for all distances from the pumped well. The nonapplicability of the Theis solution in early test times for short distances from the pumped well has also been noted previously by Hantush (1964).

Standard methods used to analyze constant-rate pumping tests that are conducted in nonleaky confined aquifers include both log-log type-curve matching, using type-curves based on the relationship presented in Theis (1935), and semi-log straight-line methods that apply after infinite-acting, radial flow conditions are established.

In ground-water hydrology, the log-log type-curve method is normally reserved for analyzing observation well response (both individually and

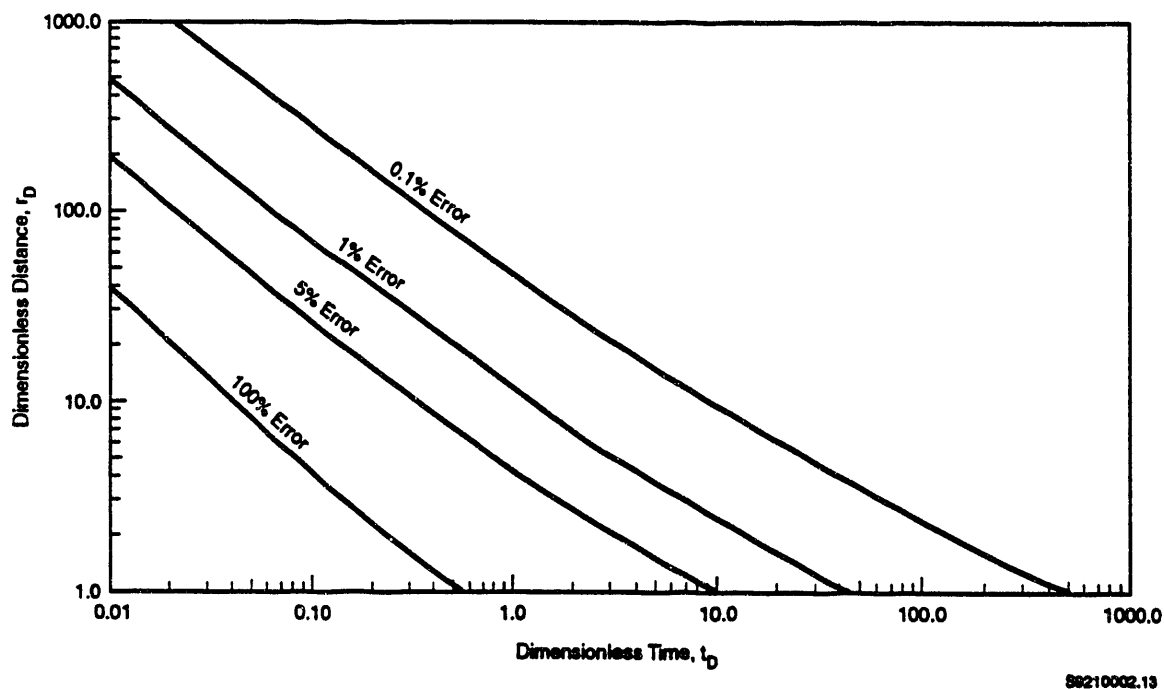


FIGURE 3.2. Error Induced by Using the Theis Solution for Various Dimensionless Distances (adapted from Mueller and Witherspoon 1965)

collectively). Log-log methods are not normally used for quantitative analysis of the pumped well, because part of the drawdown or recovery water-level response at the well location is associated with well/formation inefficiencies or damage induced by the drilling process. In the petroleum industry, the effects of well/formation inefficiencies or damage are combined and referred to as "skin effect." In petroleum reservoir analysis procedures, storativity (S), is independently estimated for the test formation, and transmissivity (T), and skin effect (s_k) are calculated simultaneously by matching the log-log drawdown or recovery response with appropriate type curves for various skin effect conditions.

For semi-log analysis methods, the rate-of-change of water levels within the well during drawdown and/or recovery is analyzed to provide hydraulic property estimates. Because skin effects are constant with time during constant-rate tests, semi-log methods can be used to quantitatively analyze the water-level response at both pumped and observation wells. In groundwater hydrology, the semi-log, straight-line analysis techniques commonly used are based on either the Cooper and Jacob (1946) method (for drawdown analysis) or the Theis (1935) recovery method (for recovery analysis). These methods are theoretically restricted to the analysis of test responses from wells that fully penetrate nonleaky, homogeneous, isotropic confined aquifers. For these analysis methods, drawdown or recovery (i.e., residual drawdown) water-level data are plotted versus the log of time or other appropriate time parameter, and T is calculated using one of the following two equations:

$$T = (2.3 Q)/(4\pi \Delta h/\Delta \log t) \quad (\text{drawdown analysis}) \quad (3.7)$$

$$T = (2.3 Q)/[4\pi \Delta s/\Delta \log (t/t')] \quad (\text{recovery analysis}) \quad (3.8)$$

where Q = pumping discharge rate [L^3/T]

Δh = water-level change [L]

Δs = residual drawdown [L]

t = time since pumping started [T]

t' = time since pumping terminated [T].

The straight-line solutions represent an approximation of the general equation describing radial flow to a well, and are valid only after a specified period of time and after infinite-acting, radial flow conditions have been established within the test formation. Infinite-acting, radial flow conditions are indicated during testing when the change in pressure, at the point of observation, increases in proportion to the logarithm of time.

Lohman (1972) indicates that the time required for the straight-line approximation to be valid (mathematically) can be calculated from the following:

$$t \geq (r^2 S)/(4T u) \quad (3.9)$$

where r is observation distance from the pumped well [L], and u is 0.01 [dimensionless].

The assigned value for u of 0.01 is somewhat conservative. Chapuis (1992) states that the

"... Cooper-Jacob approximation may be considered valid for u values higher than 0.01, as usually quoted: when $u = 0.10$, the relative error is 5.4% ..., which is scarcely detectable; for $u = 0.05$, the relative error is 2.0%."

While the time required for the straight-line approximation to be valid can be calculated (assuming T and S are known a priori), determining when infinite-acting, radial flow conditions are exhibited has, in the past, been more difficult to discern. Because of these restrictions on the use of semi-log straight-line solutions, it is important that the analyses be correctly applied to only that portion of the pumping test data for which it is valid (i.e., homogeneous formation - radial flow conditions). The use of pressure derivative techniques has greatly facilitated the identification of when infinite-acting, radial flow conditions are established, and therefore, when semi-log, straight-line solutions are valid.

3.1.1 Pressure Derivative Applications

Figure 3.3 shows the pattern of dimensionless pressure (p_D) and the dimensionless pressure derivative (p_D') during a constant-rate test for a stress well that fully penetrates a nonleaky, homogeneous, isotropic confined

aquifer for various wellbore storage conditions (i.e., $C_D > 0$). The p_D type curves were generated using a modified version of the program TYPCURV (Novakowski 1990), as described in Spane and Wurstner (1992). The original TYPCURV program was modified to allow increased density of generated type-curve data points, to permit use of external time or dimensionless time files, to extend the dimensionless head lower limit, and to provide additional test description information in the computer file output. The p_D' curves were produced using the generated p_D curve data as input to the DERIV program as described in Spane and Wurstner (1992). The values of C_D shown in the figure were selected to encompass the range of storativity (S) that is commonly cited for confined aquifer systems, i.e., $S = 10^{-3}$ to 10^{-5} (Heath 1983), where

$$C_D = r_c^2 / (2 r_w^2 S). \quad (3.10)$$

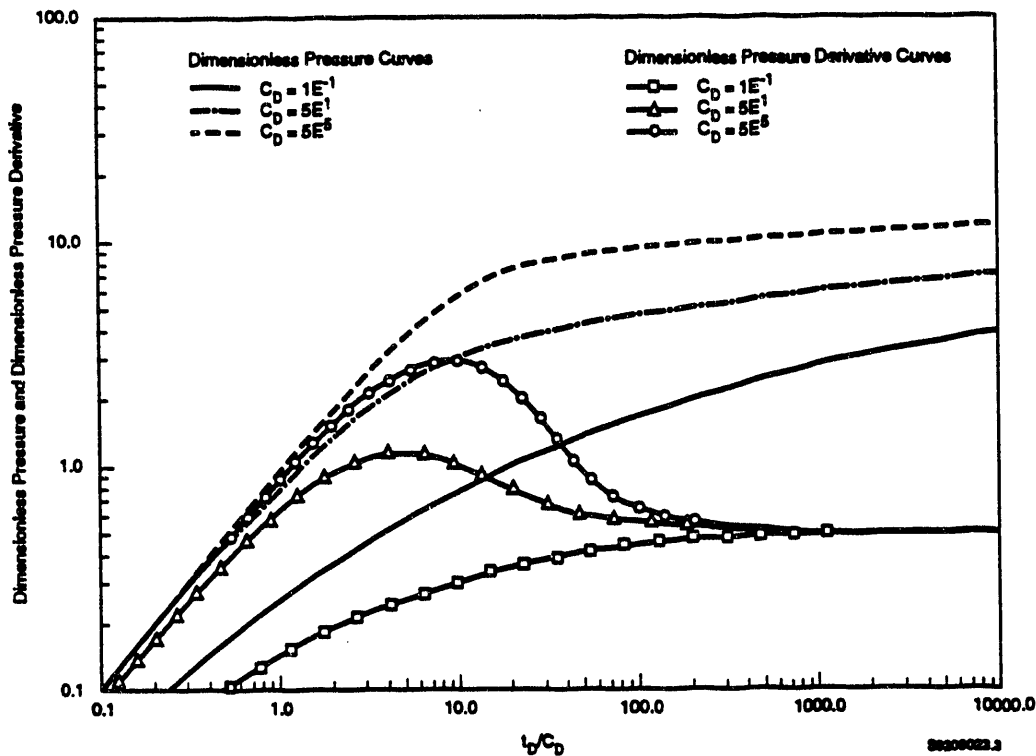


FIGURE 3.3. Dimensionless Pressure and Dimensionless Pressure Derivative Type Curves for Constant-Rate Pumping Tests

As indicated in Figure 3.3, wellbore storage produces a characteristic "hump" pattern in the pressure derivative plot, which increases in amplitude and duration as the associated dimensionless wellbore storage value (C_D), increases. A Theisian response that is characterized by no wellbore storage effects cannot be shown in the figure, because $C_D = 0$. However, because of the similarity displayed by all low C_D curves (i.e., $C_D \leq 0.1$), the absence of wellbore storage effects can be approximated by the C_D curve = 0.1 shown in the figure.

Infinite acting, radial flow conditions are indicated during testing when the change in pressure, at the point of observation, increases in proportion to the logarithm of time. This is indicated when the pressure derivative curve becomes horizontal (i.e., when the pressure derivative becomes constant) at a p_D' value equal to 0.5. For most test situations, infinite-acting, radial flow conditions are established for test times with t_D/C_D values greater than approximately 60 (Earlougher 1977).

The presence of nonradial flow conditions caused by vertical flow, leaky aquifer behavior, or the presence of boundaries is denoted on a pressure derivative plot by a diagnostic response pattern that significantly deviates from the horizontal radial flow-line region of the graph (i.e., $p_D' = 0.5$). In comparison, nonradial flow is less obvious on a dimensionless pressure change plot without the derivative. Its presence is only suggested by a subtle deviation from the pressure change plot. Figure 3.4 presents examples of diagnostic dimensionless pressure change and pressure derivative plots for a few selected heterogeneous formation test conditions. A more complete treatment of diagnostic response patterns is contained in Ehlig-Economides (1988) and Horn (1990).

3.1.2 Analysis Guidelines

The preferred analysis approach for nonleaky confined aquifers is dependent on the type of test data available for analysis. Test data may be available only from the pumped well, only one observation well, or from multiple observation wells. For the case where only drawdown data for the pumped well is available, the following analysis procedure should be used:

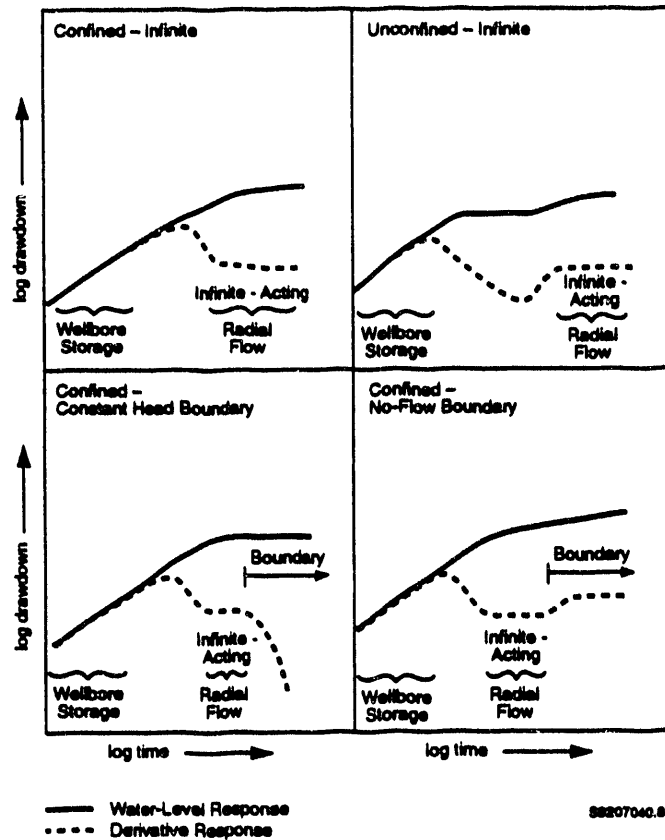


FIGURE 3.4. Characteristic Log-Log Pressure and Pressure Derivative Plots for Various Hydrogeologic Formation/Boundary Conditions

1. Plot the log of the drawdown data and data derivative versus the log of time.
2. Evaluate the drawdown data and data derivative pattern to ascertain the formation response model (i.e., homogeneous or heterogeneous), and to ascertain the presence of radial flow conditions within the test data record.
3. Calculate the transmissivity for the confined aquifer based on analysis of the indicated radial flow (if present) section of the test data using the Cooper and Jacob (1946) semi-log straight-line method [Equation (3.7)], provided that the data record analyzed satisfies the "u" time criteria listed in Equation (3.9).
4. If semi-log straight-line analysis is not applicable, then the log-log type-curve matching method (described below) should be applied.

If drawdown data are available only for one observation well, the analysis procedure outlined for the pumped well should also be followed. For this

test situation, an estimate for storativity can also be obtained from the semi-log straight-line analysis, using a modification of a relationship presented in Lohman (1972):

$$S = \frac{2.25(T t)/r^2}{\log^{-1} [(s_t)/\Delta(s/t)]} \quad (3.11)$$

where s_t is drawdown at time, t [T], and $\Delta(s/t)$ is slope of the semi-log straight-line [L/T].

In addition to the semi-log straight-line analysis procedure, simultaneous type-curve matching of the test data and data derivative can also be performed to provide corroborative estimates of transmissivity and storativity. For this analysis procedure, the Theis curve and Theis derivative (i.e., if no wellbore storage effects are exhibited) or appropriate wellbore storage and wellbore storage derivatives (e.g., Figure 3.3) can be used to match the combined log-log plot of the test data and data derivative. Once the best type curve and derivative match has been obtained, then associated match points for time, drawdown, dimensionless time ($1/u$ for Theis curve match, t_D for wellbore storage curve match), and dimensionless drawdown ($W(u)$ for Theis curve match, p_D for wellbore storage curve match) are determined. Transmissivity and storativity are then calculated using the match point data in the appropriate equations:

Transmissivity: Theis analysis [Equation (3.3)]; wellbore storage analysis [Equation (3.4)]

Storativity: Theis analysis [Equation (3.2)]; wellbore storage analysis [Equation (3.5)]

For the situation where multiple observation well data are available, the data for each well can be analyzed individually (as described previously) or all the test data can be analyzed compositely. If the data are analyzed compositely, the log of the test data and data derivatives should be plotted versus the log of t/r^2 rather than t . The test data and data derivatives should plot on a single type curve and derivative pattern, using the t/r^2 convention. A departure from a single analysis type-curve match would indicate heterogeneous formation conditions within the region tested, and the well

test data should then be analyzed individually. Transmissivity and storativity are calculated from composite analysis following the procedure outlined above for single wells, with the match point value obtained from type-curve matching as t/r^2 , instead of t .

The entire preceding discussion and discussion within Sections 3.2 and 3.3 pertains to the analysis of drawdown data obtained during constant-rate discharge tests. Recovery data for constant-rate tests can also be analyzed using drawdown type curves presented in Figures 3.3 through 3.7, provided that the recovery buildup pressure (i.e., the observed formation pressure during recovery minus the observed formation pressure at the termination of testing) are plotted versus the equivalent time function described in Agarwal (1980). The Agarwal equivalent time function accounts for the duration of the discharge time period, thereby permitting the use of drawdown type curves for the analysis of recovery data. The equivalent time function (t_e) is defined in Agarwal (1980) as

$$t_e = (t \times t') / (t + t') \quad (3.12)$$

where t is duration of the discharge test [T], and t' is time since discharge terminated [T].

Diagnostic log-log derivative analysis of recovery buildup data for identifying the establishment of radial flow conditions during the test is performed as described previously for drawdown test data analysis. The indicated radial flow portion of the recovery data can then be analyzed using semi-log recovery methods. There are several semi-log analysis methods that can be employed. The preferred analysis is based on the Theis recovery method, which analyzes residual drawdown (i.e., static formation pressure prior to test initiation minus observed formation pressure during recovery, as expressed in Equation (3.8)). Semi-log, straight-line analysis can also be performed using recovery buildup data versus the Agarwal equivalent time function (t_e) using a modified version of Equation (3.7). For this application, t_e is used in place of the indicated drawdown time (t).

As a cautionary note, semi-log straight-line analysis based on recovery buildup data versus actual recovery time (t') may provide erroneous results. This is because this analytical method assumes that drawdown has completely stabilized prior to termination of pumping. Since stabilized drawdown conditions rarely are established prior to test termination, semi-log analysis of recovery data based on the recovery time t' method should not be used.

3.2 LEAKY CONFINED AQUIFERS

Two general solutions are available for constant-rate tests conducted under leaky aquifer conditions: the Hantush and Jacob (1955) solution for which confining layer storage does not contribute a significant percentage of ground water flow to the aquifer, and the Hantush (1960) solution that includes confining layer storage effects. Both techniques retain the assumptions reported for the nonleaky case, with these additional assumptions:

1. There is no drawdown within adjacent aquifers during pumping.
2. Ground-water flow is horizontal in the pumped aquifer and vertical in the adjoining confining layers.

In addition to these two general solutions, it should also be noted that Neuman and Witherspoon (1972) provide a special test case analysis method for constant-rate tests conducted in leaky aquifer systems when drawdown data are available for both the pumped aquifer and adjacent confining layers. However, because hydraulic tests rarely have the benefit of such well deployment (i.e., except for tests specifically designed for the purpose of determining confining layer vertical hydraulic conductivity), their test analysis method will not be discussed in this report. For tests of this nature, the reader is referred to their paper, which contains an actual field test application.

3.2.1 Leaky Conditions with Confining Layer Storage

Drawdown for constant-rate tests conducted in leaky confined aquifers exhibiting significant confining layer storage is defined by Hantush (1964) as:

$$s = \frac{Q H(u, \beta)}{4 \pi T} \quad (3.13)$$

$$\text{where } \beta = r [K'S'/b'TS]^{1/2} + (K''S''/b''TS)^{1/2} / 4 \quad (3.14)$$

K = hydraulic conductivity of the overlying (') and underlying (") confining layers [L/T]

S = storativity of the overlying (') and underlying (") confining layers [dimensionless]

b = thickness of the overlying (') and underlying (") confining layers [L].

Figure 3.5 shows dimensionless drawdown, $H(u, \beta)$, versus dimensionless time (t_D) type curves for leaky confined aquifers with confining layer storage for selected β values listed in Hantush (1964). As indicated in the figure, the Theis curve represents the special condition where $\beta = 0$. It should be noted that when $\beta = 0$, dimensionless drawdown is equivalent to twice the dimensionless pressure, p_D , which is defined in Equation (3.4).

The β type curves shown in Figure 3.5 are valid for test times (t) where $t < (b'S'/10 K') + (b''S''/10 K'')$. As an assessment of this equation's range of application, if it is assumed that the thickness of the confining layers is 10 m, with a storativity of 10^{-3} and a vertical hydraulic conductivity of 1×10^{-5} m/d, then Equation (3.13) would be applicable for a test period of 50 d. A more in-depth discussion concerning the inherent assumptions of this analysis method, and applicable equations for analyzing late-time data analysis for which Equation (3.13) is not valid, is provided in Neuman and Witherspoon (1969), Reed (1980), and Molz et al. (1990).

As noted previously by Reed (1980), there is considerable uncertainty in selecting the correct β type curve for test analysis, because they are represented by a family of type curves whose shapes change only gradually with β . This uncertainty, however, is significantly reduced when the drawdown derivative curves are used simultaneously in the curve matching. As indicated in Figure 3.6, the derivative curves calculated for the β type curve values (Figure 3.5), exhibit significantly greater variability in their overall shape. As also indicated in Figure 3.6, the leaky aquifer derivatives

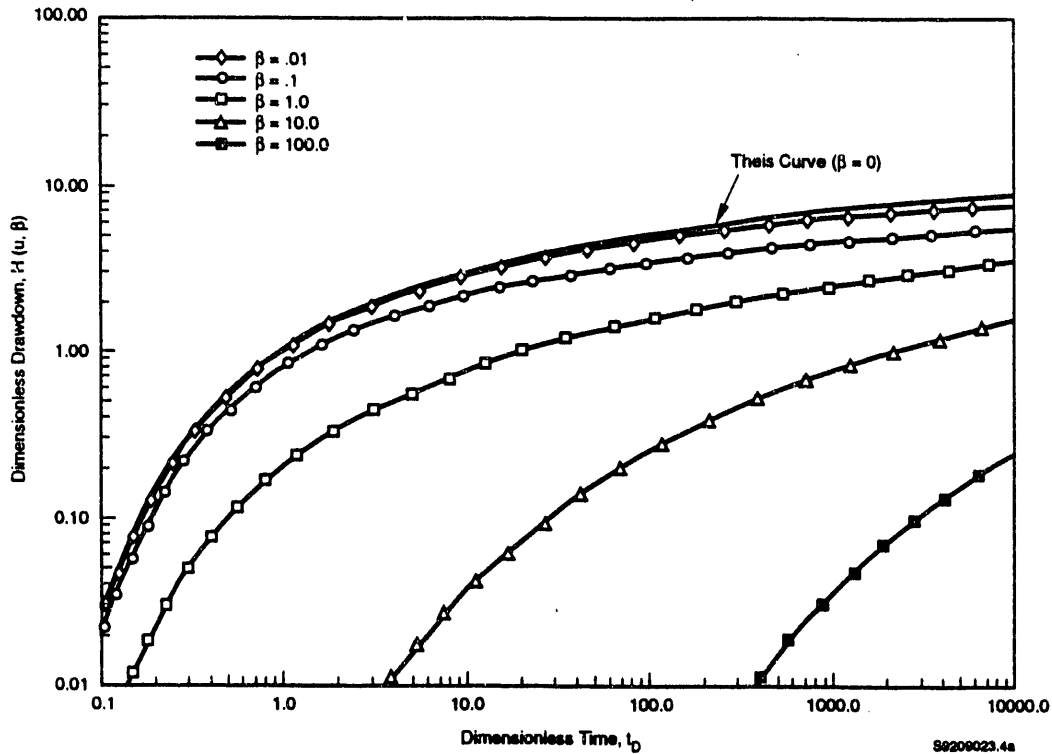


FIGURE 3.5. Dimensionless Drawdown Type Curves for Constant-Rate Discharge Tests in Leaky Confined Aquifers with Confining Layer Storage

converge in later dimensionless time to a dimensionless drawdown derivative value that is one half that of the Theis drawdown derivative [(Note: when $\beta = 0$, $H(\mu, \beta)' = 2p_D'$)].

3.2.2 Leaky Conditions Without Confining Layer Storage

For constant-rate tests conducted in leaky confined aquifers exhibiting no significant confining layer storage, drawdown is defined by Hantush (1964) as:

$$s = \frac{Q W(u, r/B)}{4 \pi T} \quad (3.15)$$

where $B = [T b' / K']^{1/2}$

b' = thickness of confining layer [L]

K' = vertical hydraulic conductivity of confining layer [L/T].

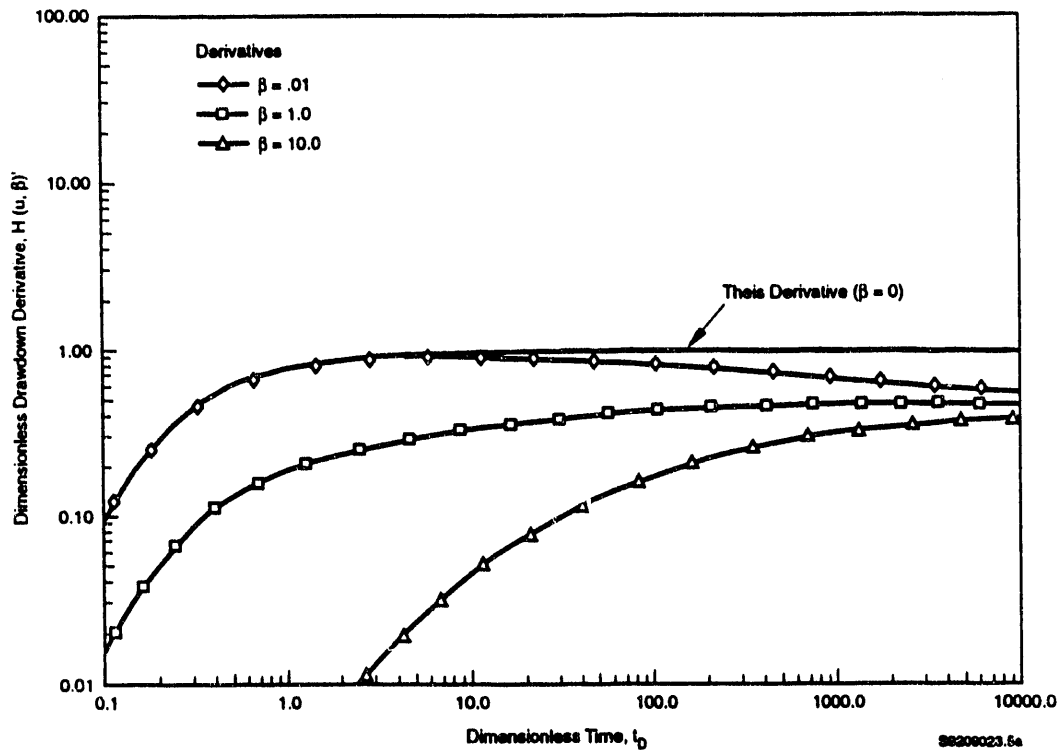


FIGURE 3.6. Dimensionless Drawdown Derivative Type Curves for Constant-Rate Discharge Tests in Leaky Confined Aquifers with Confining Layer Storage

In the hydrological sciences, Equation (3.15) is commonly referred to as the "r/B solution" method, with parameter B referred to as the "leakage factor." Weeks (1978) states that the equation is applicable for test times given by $t > (5 b'S')/K'$, where S' is the storativity of the confining layer. This time constraint indicates that this solution method is applicable for test conditions bounded by relatively thin confining layers of high hydraulic diffusivity (K'/S'). As an example of the equation's range of application, for a confining layer thickness of 3 m, storativity of 10^{-5} , and a vertical hydraulic conductivity of 1×10^{-4} m/d, the r/B solution [Equation (3.15)] would be applicable after a test period of 0.1 d. It should also be noted, however, that Neuman and Witherspoon (1969) indicated that the cited equation of applicability is too restrictive, and that the "r/B solution" method provides reasonable results over a greater range than originally indicated.

Dimensionless drawdown, $W(u,r/B)$, and drawdown derivative type curves for leaky confined aquifer conditions without significant confining layer

storage are shown in Figure 3.7. As indicated in the figure, the Theis curve and Theis derivative represent the special condition where $r/B = 0$. Unlike derivative curves developed for leaky aquifer conditions where confining layer storage is important, derivative curves developed for leaky aquifer conditions where confining layer storage is not significant display more diversity in curve shape and size. The difference in derivative curve shape greatly facilitates the selection of the correct r/B curve; particularly when used in combination with the associated drawdown curves. The uniqueness of combined drawdown and drawdown derivative curves for selected r/B values is shown in Figure 3.7.

Leaky confined aquifer derivative plots shown in Figures 3.6 and 3.7 that are coincident with the Theis derivative indicate restricted conditions for which nonleaky confined aquifer methods can be applied. As indicated in the figures, for early dimensionless times, nonleaky confined aquifer methods

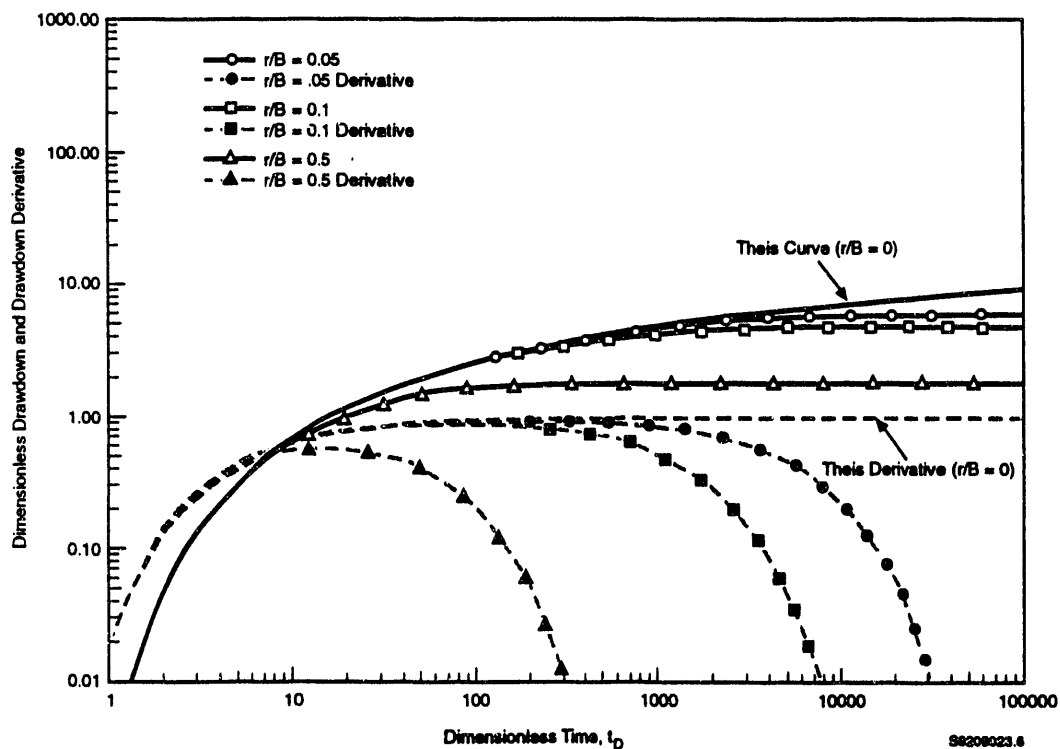


FIGURE 3.7. Dimensionless Drawdown and Dimensionless Drawdown Derivative Type Curves for Constant-Rate Discharge Tests in Leaky Confined Aquifers Without Confining Layer Storage

can be applied to leaky confined aquifer test data for test sites with β values ≤ 0.01 (for leaky aquifers with significant confining layer storage) or r/B values of ≤ 0.1 (for leaky aquifers without significant confining layer storage).

As noted previously by Lohman (1972), the selection of the appropriate drawdown type curve has relied primarily on a thorough knowledge of the geology, including the nature of the confining beds, to indicate which of the confined aquifer type curves to use for test analysis. However, as demonstrated by comparing Figures 3.3, 3.6, and 3.7, the distinctive shape of the derivative curves helps in identifying the operative confined aquifer test condition.

3.2.3 Analysis Guidelines

Quantitative analysis of leaky confined aquifer test data for pumped well, observation well, and multiple observation wells follows the same general procedures as outlined in Section 3.1 for nonleaky conditions and begins with an initial diagnostic log-log plot of the test data and data derivative. Diagnostic analysis indicates whether radial flow conditions exist in any of the test data record and, therefore, whether semi-log straight-line analysis can be performed. As indicated in Figures 3.6 and 3.7, radial flow conditions for leaky confined aquifer response would not be expected except for β values (i.e., for confining layer storage conditions) < 0.01 and r/B values (i.e., for no confining layer storage conditions) ≤ 0.1 . Because of these restrictive conditions, most leaky confined aquifer tests can only be analyzed using type-curve analysis methods.

To perform type-curve analysis, the combined drawdown type curve and derivative plots shown in Figures 3.5, 3.6, and 3.7 are superimposed on the log-log plot of the test data and data derivative. As discussed previously, the distinctive shape of the drawdown derivative helps identify the operative leaky aquifer condition, i.e., the β or r/B solution method. After the best type curve and derivative match has been obtained, then associated match points are selected for time (t), drawdown (s), dimensionless time (t_D), and dimensionless drawdown ($H(u,\beta)$ for leaky/with confining layer storage; $W(u,r/B)$ for leaky/without confining layer storage). Transmissivity, stora-

tivity, and other hydraulic properties can then be calculated using the match point information in the appropriate equations that follow:

Leaky/With Confining Layer Storage

Transmissivity: Use match point values for $H(u,\beta)$ and s in Equation (3.13).

Storativity: Use calculated transmissivity and match point values for t and t_D in Equation (3.5).

Confining Layer Use calculated values for transmissivity and storativity, and match curve β value in Equation (3.14) to estimate the combined vertical hydraulic diffusivity of the confining layers.

Leaky/Without Confining Layer Storage

Transmissivity: Use match point values for $W(u,r/B)$ and s in Equation (3.15).

Storativity: Use calculated transmissivity and match point values for t and t_D in Equation (3.5). For the case where $S' < 0.01S$, Hantush (1960) states that u should be replaced by $u(1+S'/3S)$. This causes a further modification to Equation (3.5) to $t_D = (T)/(r^2 S)(1+S'/3S)$.

Confining Layer Properties: Use calculated value for transmissivity, the match curve value for B (i.e., for the given r distance value), and the known confining layer thickness (b') in Equation (3.16) to estimate the confining layer vertical hydraulic conductivity.

For leaky aquifer test analysis in the situation where multiple observation well data are available, the well test data can be analyzed individually (as described previously) or compositely. If the data are analyzed compositely [as suggested by Weeks (1978)], the added constraint should be added that distance (r) values for the observation wells must fall on type curves with proportional β (for leaky/with confining layer storage) or r/B values (for leaky/without confining layer storage). A deviation from this proportionality constraint would indicate heterogeneous formation conditions within the region tested, and the well test data should then be analyzed individually.

3.3 UNCONFINED AQUIFERS

Important contributions in the development of analysis methods for constant-rate discharge tests conducted within unconfined aquifers include: Boulton (1954, 1963), Dagan (1967), Streltsova (1972 and 1973) and Neuman (1972, 1973, 1974, and 1975). A detailed summary and discussion of these methods are presented in the cited Neuman references. Because of its rigorous basis on physical principles, which permits a complete description of unconfined aquifer response, the solution method presented in Neuman (e.g., 1975) is used and discussed in this report. As shown in Neuman (1974, 1975, and 1979), the analytical results obtained by Boulton, Dagan, and Streltsova methods represent special unconfined aquifer response conditions that can be duplicated with the more complete and rigorous solution presented in the Neuman references. The historical background and development of constant-rate test analysis within unconfined aquifers is not presented in this report. For a discussion on this topic, the reader is directed to the cited references.

As background for the discussion pertaining to unconfined aquifer test analysis, it is beneficial to briefly examine the characteristic differences between unconfined and confined aquifer test response. For confined aquifers, ground water is released from elastic storage (including expansion of water and compression of the aquifer matrix), while for unconfined aquifers ground water is produced from both elastic storage and by gravity drainage from the lowering water-table surface. As test time increases, the elastic storage (i.e., storativity S), response becomes less important within the unconfined aquifer, with ground-water production being controlled largely by its specific yield (S_y). The elastic storage response during constant-rate tests conducted within unconfined aquifers has been documented previously by Gambolati (1976) and Neuman (1974, 1979). Another difference is that for unconfined aquifers, the upper flow boundary (i.e., water table) is not fixed as is the case with confined aquifers.

3.3.1 Unconfined Aquifer - Type Curve Analysis

Because unconfined aquifers produce ground water from two sources of storage and the water table is not fixed during testing, unconfined aquifer pumping tests depart from those predicted by the Theis equation. Walton

(1960) states that unconfined aquifer constant-rate discharge tests conducted within fully penetrating wells are characterized by the presence of three distinct segments on a time-drawdown curve. In the first segment, the aquifer reacts as would a confined aquifer, with ground water produced through the expansion of water and compaction of the aquifer matrix. Drawdowns during this segment follow those predicted using the Theis equation, with aquifer storage equal to its elastic storativity component (S). During the second segment of the drawdown curve, the rate of drawdown decreases as gravity drainage (i.e., vertical ground-water flow components) becomes important within the aquifer. Gravity drainage (also referred to as delayed yield) within the unconfined aquifer causes the time-drawdown curve to deviate significantly from that predicted by the Theis equation, since the gravity drainage/vertical ground-water flow components "reflect the presence of recharge in the vicinity of the pumped well" (Walton 1960). During the third segment, gravity drainage effects become insignificant, and radial flow conditions are once again predominant within the aquifer. Drawdowns during this segment once again follow those predicted using the Theis equation, with aquifer storage equal to its combined elastic storativity component (S) and specific yield (S_y).

The influence and duration of the first two segments of the time-drawdown curve are reported by Neuman (1972) to be largely controlled by the parameter $\sigma = S/S_y$. The smaller the value of σ , the more pronounced the effects of gravity drainage (i.e., the second segment) become. As σ approaches 0, the first segment disappears, leaving only the second and third segments of the curve. Conversely, as σ approaches infinity, the second segment vanishes and the third segment becomes coincident with the first segment of the time-drawdown curve. Figure 3.8 shows the dimensionless time-drawdown response within an unconfined aquifer for a given input parameter value of $\sigma = 10^{-3}$, for a selected range of β values, where β is defined by Neuman (1972) as:

$$\beta = K_0 (r^2/b^2) \quad (3.17)$$

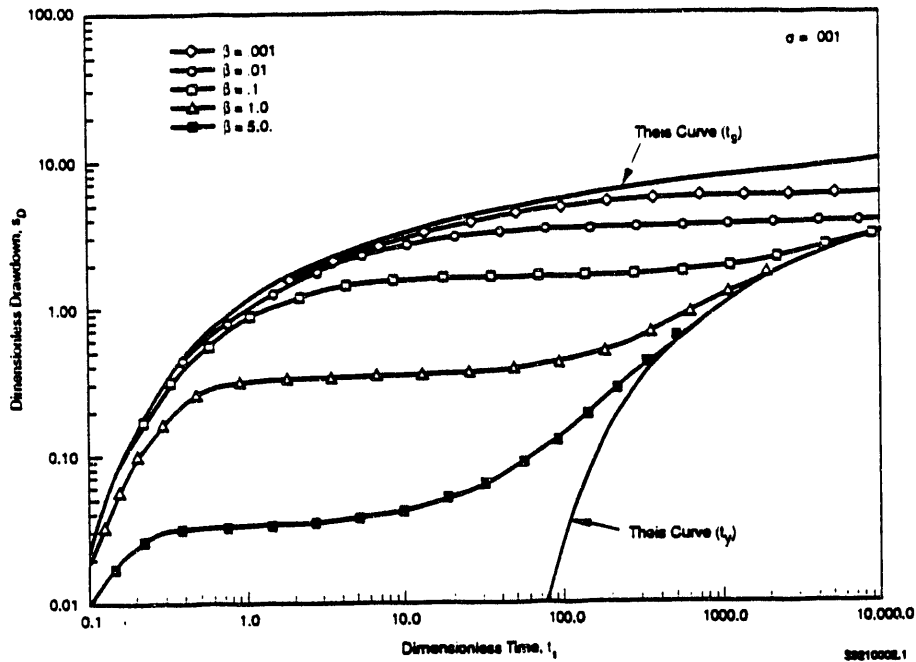


FIGURE 3.8. Dimensionless Time-Drawdown Type Curves for Constant-Rate Discharge Tests in Unconfined Aquifers for $\sigma = 10^{-3}$

where K_D is ratio of vertical to horizontal hydraulic conductivity, K_v/K_h [dimensionless], and b is aquifer thickness [L].

Because of the variability of the parameter σ , a universal set of diagnostic log-log type curves and associated derivatives cannot be developed that describe complete unconfined aquifer test response during constant-rate testing. Drawdown derivative curves can be developed, however, that describe the first and second segments and second and third segments of the unconfined aquifer flow response, using the $W(u_A, \beta)$ and $W(u_B, \beta)$ type-curve relationships presented in Neuman (1975). Figures 3.9 and 3.10 show dimensionless drawdown type-curve patterns for the first and second segments (Neuman type A curves) and the second and third segments (Neuman type B curves) of unconfined aquifer test response behavior. Their associated drawdown derivative type curves are presented in Figures 3.11 and 3.12, respectively.

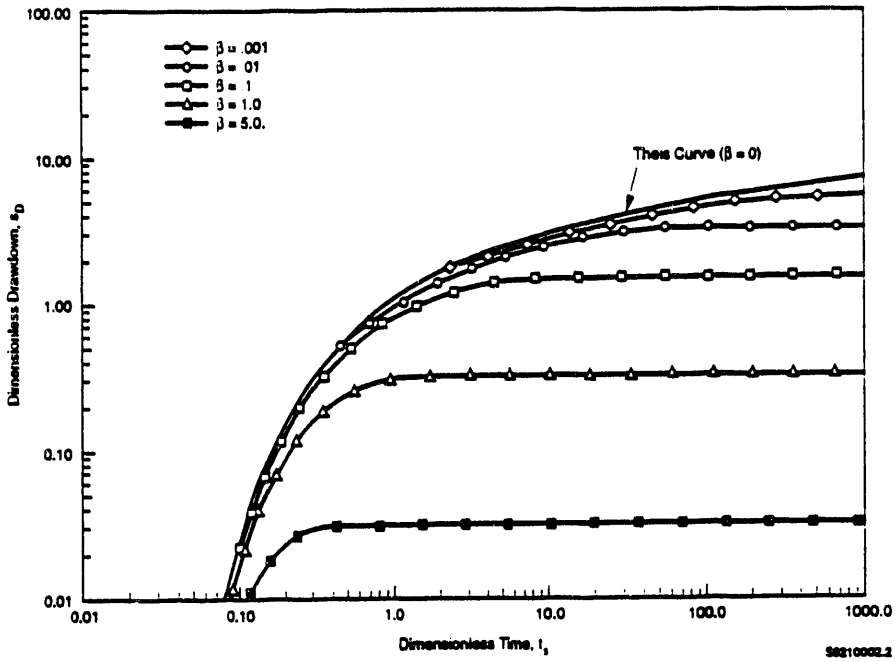


FIGURE 3.9. Dimensionless Drawdown Type Curves for Constant-Rate Discharge Tests Unconfined Aquifer Delayed-Yield (Neuman) Type A Curves

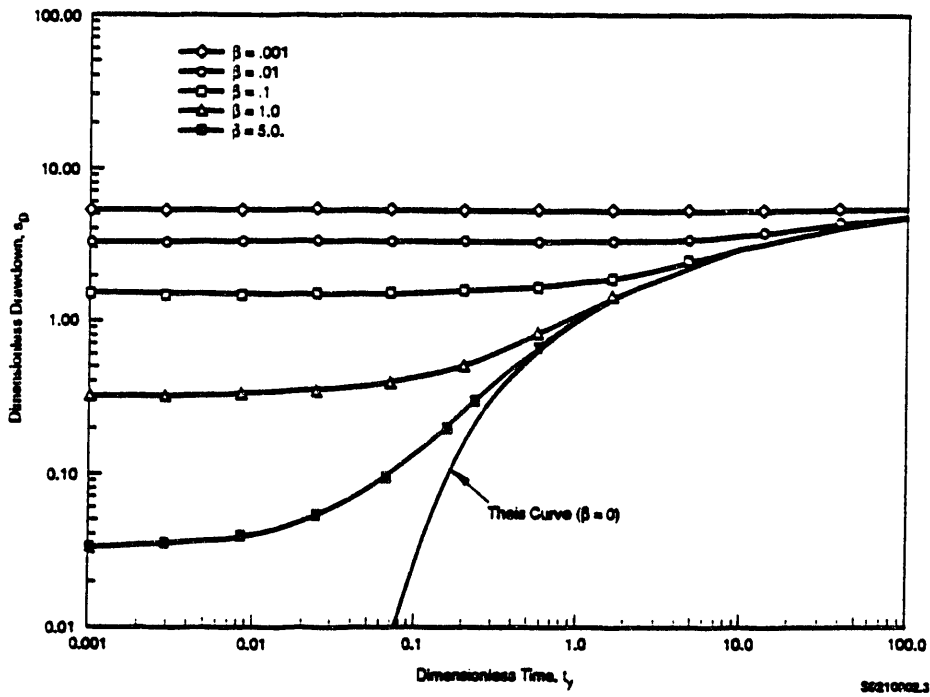


FIGURE 3.10. Dimensionless Drawdown Type Curves for Constant-Rate Discharge Tests Unconfined Aquifer Delayed-Yield (Neuman) Type B Curves

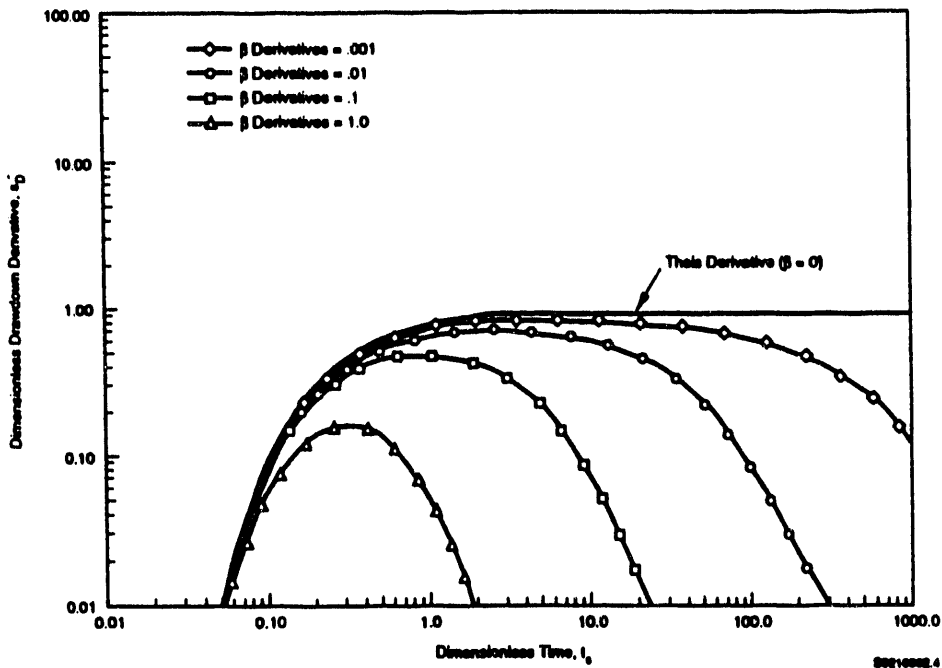


FIGURE 3.11. Dimensionless Drawdown Derivative Type Curves for Constant-Rate Discharge Tests Unconfined Aquifer Delayed-Yield (Neuman) Type A Curves

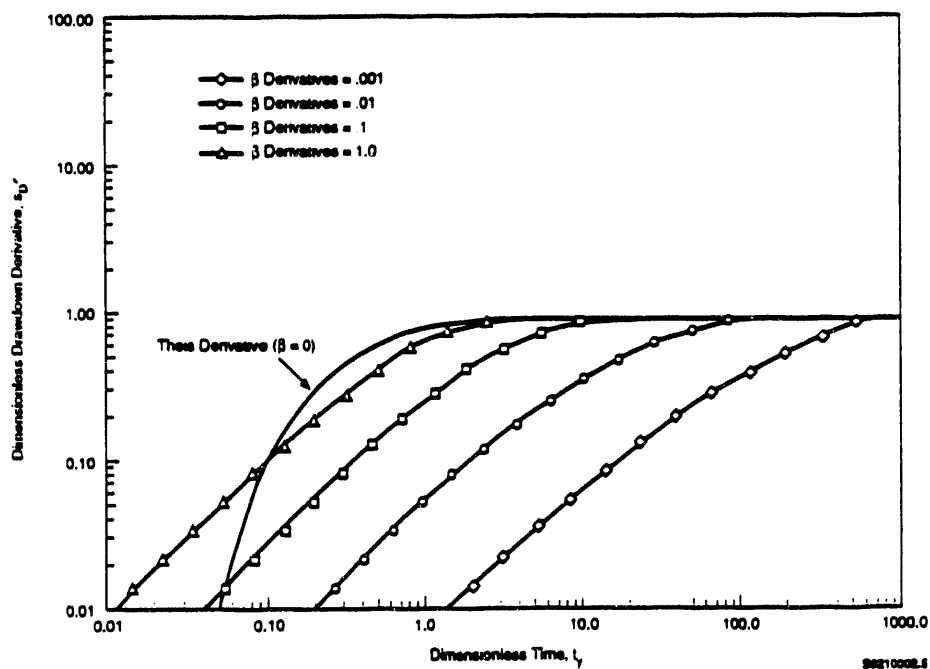


FIGURE 3.12. Dimensionless Drawdown Derivative Type Curves for Constant-Rate Discharge Tests Unconfined Aquifer Delayed-Yield (Neuman) Type B Curves

The dimensionless time parameters (t_s and t_y) shown in the figures are variants of the general dimensionless time parameter [t_D Equation (3.5)], and are defined as:

$$t_s = (T t)/(r^2 S) \quad (3.18)$$

$$t_y = (T t)/(r^2 S_y) \quad (3.19)$$

The dimensionless drawdown, s_D , is defined as:

$$s_D = \frac{4\pi T \Delta h}{Q} \quad (3.20)$$

Figures 3.9 and 3.11 show an overall degree of similarity between individual Neuman type A dimensionless drawdown type curves and individual drawdown derivatives. However, when used in combination, a distinctive type-curve and derivative pattern is indicated, which greatly facilitates the selection of the correct beta curve value that is used in matching the combined observed test data and data derivative.

Once the best beta curve match has been obtained by using the combined type curve and derivative match approach, associated match points for time and dimensionless time (t_s for type A curves and t_y for type B curves) and drawdown and dimensionless drawdown (s_D) are obtained. The match-point values for drawdown and dimensionless drawdown are used in Equation (3.20) to obtain an estimate for transmissivity. The calculated transmissivity estimate is then used with the match point values for time and dimensionless time in the appropriate dimensionless time equation [i.e., Equation (3.18) or (3.19)] to provide an estimate for either S or S_y . An estimate for the vertical hydraulic conductivity anisotropy ratio (K_D) can also be obtained using the value for beta obtained from the type curve/ derivative match in the relationship presented in Equation (3.17). An estimate for vertical hydraulic conductivity (K_v) can also be obtained from the calculated K_D value if the aquifer thickness is known (note: $K_h = T/b$).

It should be noted that the Neuman type A dimensionless drawdown curves (Figure 3.9) and associated derivative patterns are very similar to those exhibited by leaky confined aquifer conditions without significant confining layer storage (Figure 3.7). The similarity in derivative patterns is expected, given the overall similarity exhibited by the dimensionless drawdown type-curve patterns. The similarity between dimensionless drawdown type-curve patterns for unconfined aquifers (i.e., Neuman type A) and leaky confined aquifers with significant confining layer storage was also noted previously by Neuman (1975). Distinguishing between operative aquifer conditions at a test site (i.e., unconfined versus confined) may be ascertained by evidence from existing hydrogeologic data, confined aquifer responses to external loading phenomena (e.g., barometric efficiencies), and/or extending test durations a sufficient length of time to show whether late-time test responses demonstrate third segment unconfined aquifer response behavior (i.e., late-time Theisian behavior).

3.3.2 Confined Aquifer Solution Analysis

In addition to improving the log-log type-curve matching of unconfined aquifer test data analysis, pressure derivative analysis can also be employed to establish when, or if, infinite-acting, radial flow conditions have been established during the first or third segments of the unconfined aquifer response curve, thereby verifying the use of semi-log, straight-line analysis for these test data segments. If radial flow conditions are indicated within the test data record, procedures described in Section 3.1 for nonleaky confined aquifer analysis can be employed for the determination of transmissivity and storativity. To analyze unconfined aquifer test results with confined aquifer straight-line solutions, the drawdown data must be corrected for the effects of aquifer dewatering. Jacob (1963) states that when drawdown (s) represents a significant percentage of the original aquifer thickness, then drawdown data should be reduced by the factor $s^2/2b$, where b equals the aquifer's original saturated thickness. As noted by Neuman (1975), this correction should only be implemented for late-time drawdown data (i.e., during the third segment of unconfined aquifer response behavior).

4.0 FACTORS AFFECTING HYDRAULIC TEST ANALYSIS

As mentioned previously, standard log-log and semi-log analysis methods used in the interpretation of constant-rate discharge tests depend on assumed Theisian well/formation conditions such as a homogeneous, isotropic aquifer of infinite lateral extent; fully penetrating/communicative wells possessing infinitesimally small borehole volumes; and radial flow conditions. It is important that when these conditions and assumptions are not met, the significance on constant-rate discharge test response be understood.

This section examines the effects of selected factors that commonly influence the performance of constant-rate discharge tests. The selected factors are grouped into three categories: factors that pertain to well construction conditions, factors that relate to formation heterogeneities, and extraneous stresses.

4.1 WELL CONSTRUCTION CONDITIONS

Well construction conditions can influence the performance of constant-rate discharge tests in several ways. As noted earlier, the analytical methods based on type-curve matching and straight-line analysis assume that the wellbore volume does not contribute water during the course of the test (i.e., no wellbore storage); the well is in complete communication with the test formation, with no significant well friction losses during testing (i.e., no well damage); and the pumping and observation wells fully penetrate the aquifer. The fact that these conditions commonly do not occur during field tests necessitates an examination of their impact on the previously discussed type-curve and straight-line analysis methods.

4.1.1 Wellbore Storage

The changing water level in a finite volume wellbore during a constant-rate test implies that a certain percentage of the ground water produced will come from this source and not from the formation. Papadopulos and Cooper (1967) and Agarwal et al. (1969) indicated that during the early stages of a constant-rate test within a confined aquifer, wellbore storage will cause a departure in drawdown from that predicted by the Theis equation. The effect

of wellbore storage is the characteristic unit slope that is evident on a log-log plot of drawdown data versus time. The duration of the wellbore storage is a function of the ratio of wellbore storage to formation storativity and the transmissivity of the aquifer. Earlougher (1977) states that as a "rule of thumb" the time after which wellbore storage is no longer important and standard semi-log analysis methods are applicable usually occurs about 1 to $1\frac{1}{2}$ log cycles in time after the log-log data plot starts to deviate significantly from the unit slope. The time can be estimated from a modification of a relationship presented in Earlougher (1977) that indicates the establishment of radial flow conditions in an infinite, homogeneous, confined aquifer for dimensionless times, $t_D \geq 60C_D$. Substituting this relationship in Equation (3.5) and combining it with Equation (3.10) provides a time estimate for the establishment of radial flow of $t \geq 30 r_c^2/T$. This is similar to the radial flow time criterion of $t \geq 25 r_c^2/T$ reported in Weeks (1978).

As indicated previously in Figure 3.3, the dimensionless pressure derivative exhibits a distinct "hump" pattern for wellbore storage-dominated flow, which declines with time, becoming asymptotic with the horizontal line value ($p_D' = 0.5$), which indicates establishment of radial flow conditions. As Figure 3.3 shows, wellbore storage prolongs the time required for radial flow conditions to be established. The effects of wellbore storage within the pumped well (i.e., no observation well storage) also dissipate with distance. Figure 4.1 shows that for the example examined, wellbore storage effects are still evident for distances greater than 100 wellbore diameters. However, the effects dissipate by a t_D/C_D value of about 60, as noted previously.

Constant-rate discharge test data influenced by wellbore storage can be analyzed using type-curve and derivative plots presented by Bourdet et al. (1983a, 1983b) or by generating type curves with the TYP CURV program described by Novakowski (1990). Corresponding derivative responses can then be produced using the program DERIV presented in Spane and Wurstner (1992). It should be noted that formation hydraulic properties cannot be determined from constant-rate test data that display purely wellbore storage effects, i.e., pressure drawdown data plotting as a unit slope and having data derivatives plotting on the rising limb of the derivative "hump"). Hydraulic properties can be

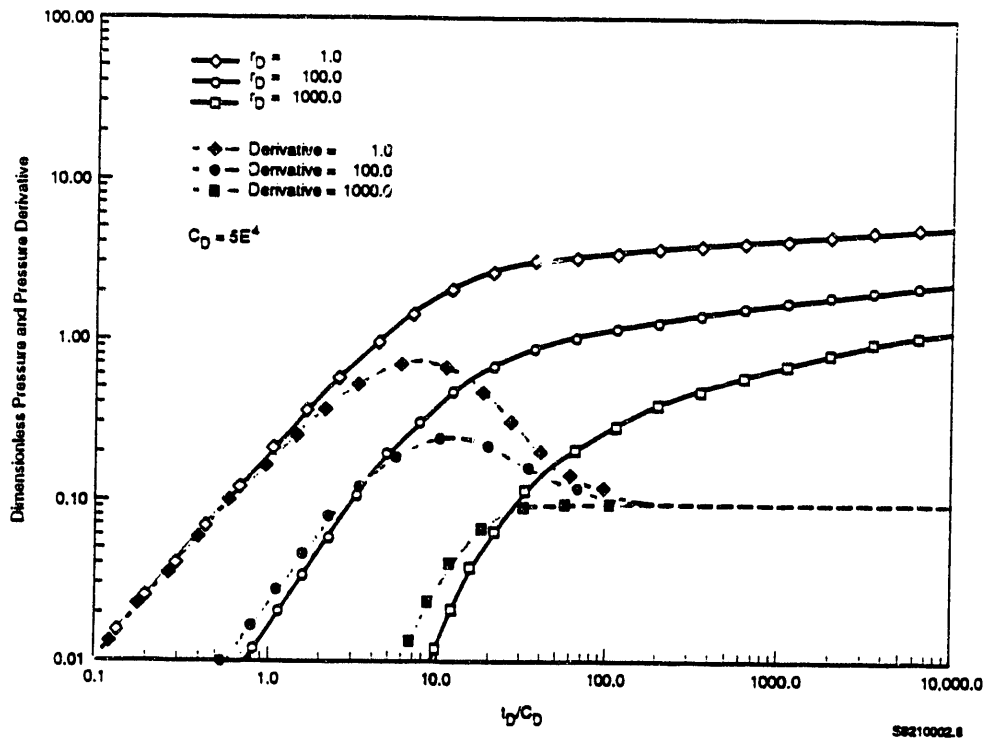


FIGURE 4.1. Effects of Wellbore Storage During Constant-Rate Discharge Tests for Selected Radial Distances

estimated using type-curve and derivative matching techniques prior to the establishment of radial flow conditions, if sufficient test data are available to describe the wellbore storage hump and declining limb region of the data derivative.

There are currently no unconfined aquifer type curves available that take observation well wellbore storage effects into account. However, wellbore storage influence would be expected to be limited to the early stages of the unconfined aquifer response (i.e., the first segment of unconfined aquifer flow), and therefore only affect unconfined aquifer test analysis using Neuman type A curves and derivatives (Figures 3.9 and 3.11). The test analysis procedure outlined in Section 3.3.1 using Neuman type B curves and derivatives should apply even if wellbore storage effects are manifest during the early stages of the test.

Wellbore storage effects do not influence the results of semi-log straight-line methods because these techniques are restricted to the analysis of test data exhibiting radial flow conditions. However, wellbore storage does cause a delay in the establishment of radial flow conditions for which straight-line analysis may be applied.

4.1.2 Wellbore Damage

Physical aspects of well construction and completion can reduce the efficiency of the well for ground-water extraction during a constant-rate test. In particular, drilling can cause a zone of lower permeability to develop within the formation around the well due to the invasion of drilling fluids containing suspended solids (e.g., rock cuttings). Poor well completion practices, such as improper well screen design and incomplete well development, can also contribute to ground-water extraction inefficiencies.

In the petroleum industry, factors contributing to well inefficiency or wellbore damage are combined and referred to as "skin effect" or "skin factor" (Ramey 1982). The skin effect (s_k) causes an additional pressure drawdown to be added to the flow equations governing ground-water flow to the pumped well during constant-rate testing. If the zone of damage is envisioned as being restricted to the wellbore surface, the skin effect is referred to as the infinitesimal thickness case. If the zone of damage extends a measurable distance into the surrounding formation, a finite thickness skin model is used in the test analysis. Figure 4.2 shows dimensionless pressure and dimensionless pressure derivative curves reported by Bourdet et al. (1983a) that describe drawdown behavior at the pumping well in the presence of an infinitesimal thickness skin. The difference between these curves and the curves presented in Figure 3.3 for wellbore storage is the added skin effect. For this situation, C_D is replaced in Equation (3.10) by the term $C_D e^{2s_k}$. As indicated in Figure 4.2, the skin effect tends to heighten the effects of wellbore storage and tends to extend the time required to reach radial flow conditions. No universal dimensionless pressure and dimensionless pressure derivatives are available for the case of a finite thickness skin. This is because a set of type curves and derivatives must be generated for each skin thickness. For

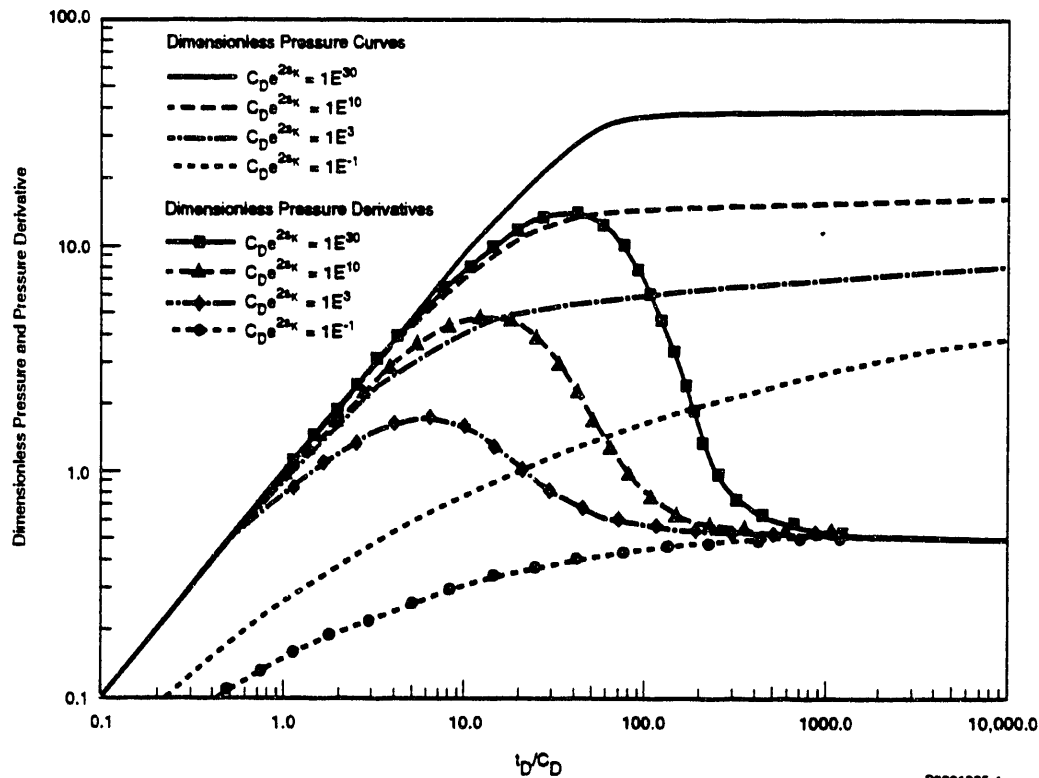


FIGURE 4.2. Dimensionless Pressure and Dimensionless Pressure Derivative Type Curves for Constant-Rate Pumping Tests (adapted from Bourdet et al. 1983a)

these situations, type curves and derivatives can be generated using the TYPCURV (Novakowski 1990) and DERIV (Spang and Wurster 1992) computer programs previously described.

Because the skin effect tends to magnify wellbore storage effects within the pumped well, the discussion presented in Section 4.1 for the impact of wellbore storage on well test analysis is also appropriate for the analysis of constant-rate test data in the presence of skin. The only difference is that dimensionless pressure and derivative curves used in the type-curve matching procedure are either as shown in Figure 4.2--for the infinitesimal skin thickness case--or generated curves and derivatives for the finite thickness skin case. In either situation, semi-log, straight-line analysis is not affected by the presence of skin, provided that only test data indicative of radial flow conditions are analyzed.

As a point of interest, the effects of wellbore damage and well inefficiency can be quantified utilizing step-drawdown testing. Drawdown caused by

well losses as determined from step-drawdown testing can then be subtracted from the observed drawdown test data obtained during constant-rate testing for the particular constant discharge rate. The corrected drawdown data can then be analyzed with the previously described test methods. The design and analysis of step-drawdown testing are not discussed in this report. The reader is referred to Rorabaugh (1953) and Lennox (1966) for a detailed discussion concerning the step-drawdown test method.

4.1.3 Partial Penetration

Partial penetration of the aquifer by the pumped well causes distortion of the radial flow/equipotential pattern that would normally develop during testing within a homogeneous, isotropic aquifer surrounding a fully penetrating stress well. To illustrate its effect, Figure 4.3 shows the areal deviation in drawdown equipotential lines and flow lines that develop during a

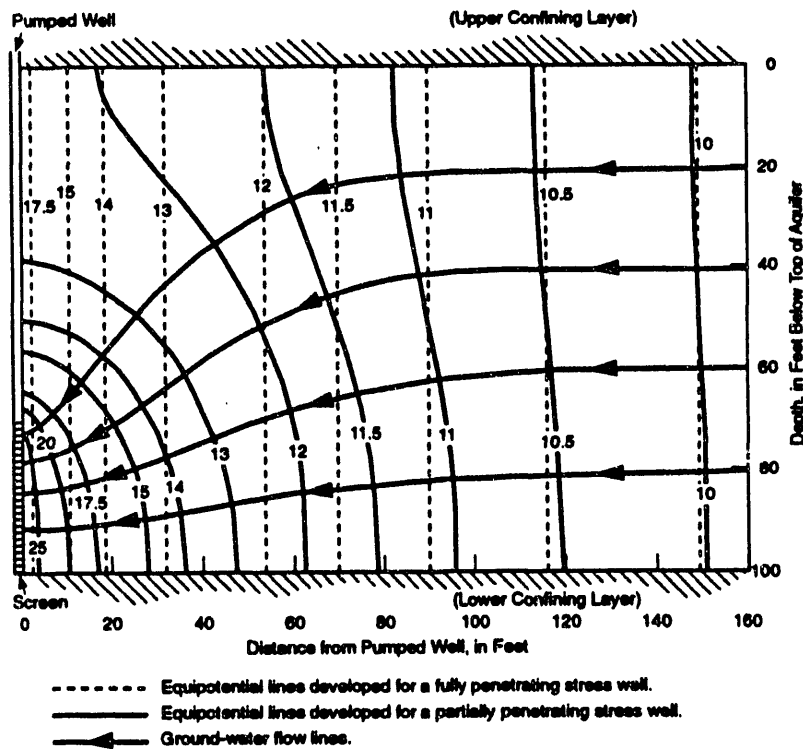


FIGURE 4.3. Effects of a Partially Penetrating Pumping Well Completed in the Lower 30% of a Confined Aquifer (adapted from Weeks 1969)

constant-rate pumping test for a stress well that penetrates the lower 30% of a confined aquifer. As shown, partial penetration effects cause more drawdown to occur within the surrounding screened depth interval section of the aquifer and less drawdown to occur within the nonscreened aquifer section (i.e., the upper 70% of the aquifer). Deviations induced by partial penetration are more significant near the stress well and diminish with distance. Hantush (1961) states that the flow pattern during testing is essentially radial for observation well distances ≥ 1.5 times the aquifer thickness; for practical purposes, equations based on fully penetrating stress wells (e.g., the Theis equation) provide sufficiently accurate results for observation well distances as small as the aquifer thickness, b (i.e., $r/b = 1$). This is valid provided that $u < 0.1 (r/b)^2$, where u is equal to $(r^2 S)/(4 T t)$ [Equation (3.1a)].

For observation wells located within a distance/aquifer thickness ratio of $r/b \leq 1.5$, the effects of partial penetration for confined aquifer tests can be accounted for following techniques presented by Weeks (1964, 1969), which are based on relationships originally presented in Hantush (1961). The corrections associated with partial penetration (s_p) are added to the drawdown equations for confined aquifers as stated in Equations (3.3), (3.13), and (3.15). For drawdown within a nonleaky confined aquifer, the equation for drawdown for partially penetrating wells is:

$$s = \frac{Q W(u)}{4\pi T} + s_p \quad (4.1)$$

$$\text{where } s_p = f_{(s)} \frac{Q}{4\pi T}$$

Equation (4.1) is valid for test times after which partial penetration is constant, which is reported by Reed (1980) for times $t > (b S)/2K_v$. The dimensionless partial penetration factor, $f_{(s)}$, can be determined from tables presented in Weeks (1969) for pumping and observation well penetration relationships or calculated directly with available computer programs that are based on equations presented in Hantush (1961), such as Reed (1980) and Walton (1987).

Because there are many various pumping and observation well configurations, a universal set of partial penetration correction types cannot be developed. Figure 4.4, however, shows the magnitude of correction for a pumping well screened over the aquifer depth interval from $0.6b$ to $0.9b$ for various piezometer depths. As indicated in the figure, additional drawdown due to partial penetration occurs for piezometer depths near the screened interval. Also shown in the figure is the verification that partial penetration effects are completely dissipated at distances of 1.5 times the aquifer thickness.

The procedures presented in Weeks (1969) are strictly applicable for confined aquifer conditions. These partial penetration procedures can, however, be applied for unconfined aquifer conditions provided that unconfined

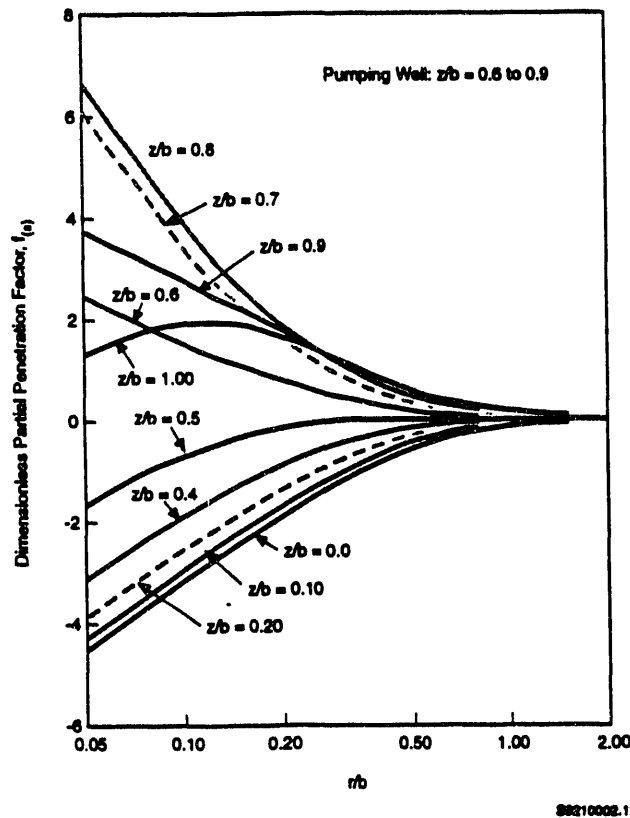


FIGURE 4.4. Partial Penetration Corrections for Selected Piezometer Depths Given a Pumping Well Screened Interval Depth, $z/b = 0.6$ to 0.9 (modified from Weeks 1969)

aquifer drawdown follows Theisian flow theory. As discussed previously (Section 3.3.1), this can occur in early- or late-time, during the first and third segments of unconfined aquifer flow. A better means of describing the effects of partial penetration on complete unconfined aquifer response behavior can be evaluated using equations and type-curve figures presented in Neuman (1972, 1973, 1974, and 1975). Figures 4.5 and 4.6 show predicted unconfined aquifer response at various piezometer depths ($z_0 = z/b$) for a fully penetrating pumping well and for a pumping well that penetrates the bottom 30% of the aquifer. The radial distance to the piezometer depths shown is equal to the aquifer thickness, i.e., $r = b$. The figures were generated using the computer program DELAY2, which is described in Neuman (1975).

Figure 4.5 shows the considerable difference exhibited in unconfined aquifer response at various depths of observation, for the case of a fully penetrating pumping well. As indicated, the piezometer depth that coincides

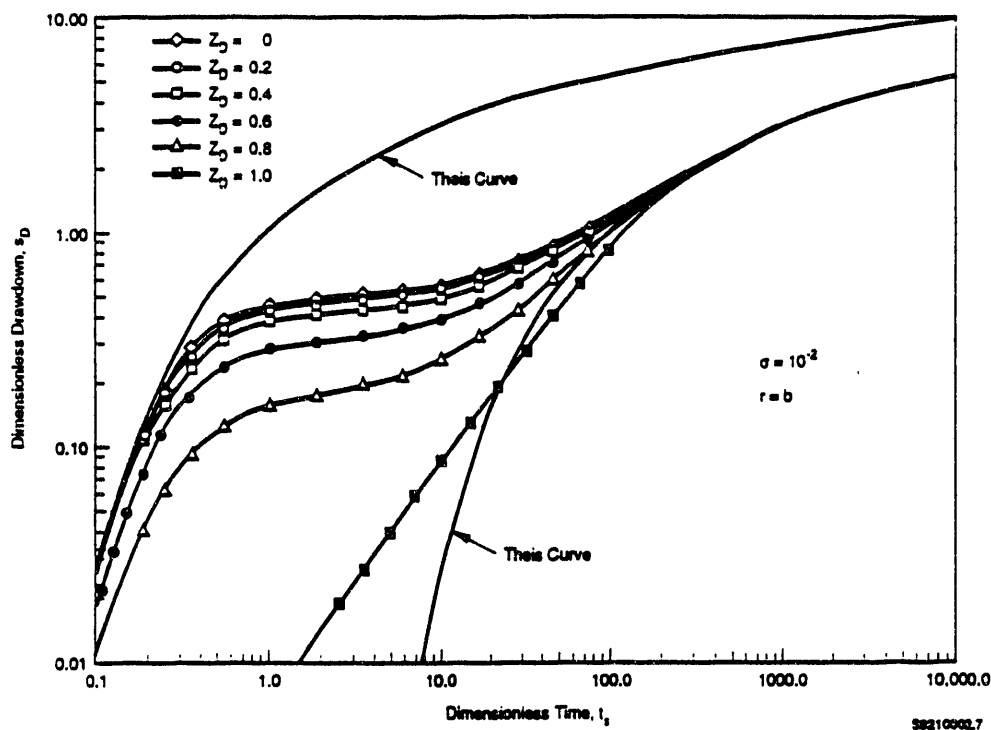


FIGURE 4.5. Characteristic Unconfined Aquifer Behavior During Constant-Rate Discharge Tests for $K_D = 1.0$; $r = b$

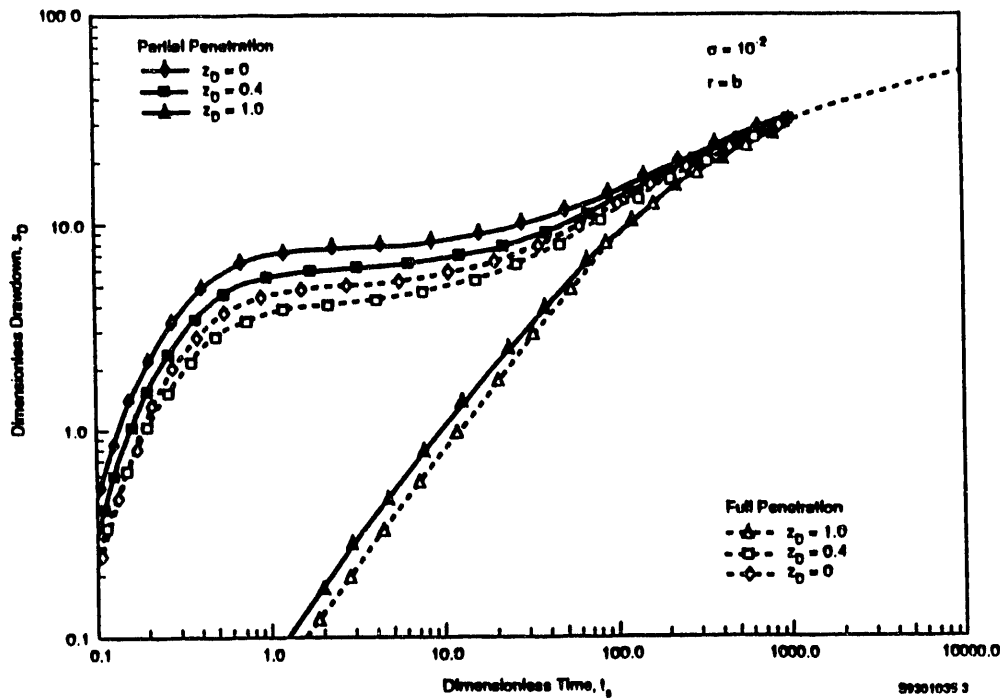


FIGURE 4.6. Effects of Partial Penetration Within an Unconfined Aquifer During Constant-Rate Testing

with the water-table surface (i.e., $z_D = 1.0$) shows a significant delay and deviation from that predicted by the Theis solution, thereby illustrating the term "delayed-yield" that characterizes unconfined aquifer flow. Figure 4.6 shows a comparison of drawdowns for a fully penetrating pumping well and a pumping well that penetrates only the lower 30% of the aquifer at selected piezometer depths. As indicated, greater drawdowns are exhibited at all piezometer depths for the partially penetrating pumping well case. As reported by Neuman (1974) and illustrated in Figure 4.6, the effects of partial penetration in an isotropic aquifer diminish with time and become coincident with the Theis equation at a dimensionless time value, $t_y \geq 10$ (i.e., $t_s \geq 1000$ for $\sigma = 10^{-2}$) for all radial distances exceeding $r/b = 1$. In addition, Neuman (1974) states that the effects of partial penetration at the pumping well can be minimized by using fully penetrating observation wells, rather

than piezometers. For these situations, pumping well partial penetration effects can be neglected at fully penetrating observation wells for all radial distances exceeding $r/b = 1$ and dimensionless times $t_y > 1$ (Neuman 1974).

In summary, partial penetration effects can be fully accounted for by generating time/drawdown, type curve responses for the specific partial penetration depths and observation well distance/depth relationships using the computer program DELAY2. Alternatively, late-time data analyses can be performed using previously discussed unconfined and confined aquifer analytical techniques for test data that follow Theisian flow behavior. For piezometers and fully penetrating observation wells at radial distances exceeding $r/b = 1$, the times required for establishing Theisian flow conditions are $t_y \geq 10$ and ≥ 1 , respectively.

4.2 FORMATION CONDITIONS

The previous discussions assume that the tested aquifer is homogeneous, isotropic, and infinite in lateral extent. In this section, the effects of aquifer heterogeneity, specifically vertical anisotropy ($K_D = K_v/K_h$), and the effects of lateral discontinuities (i.e., impermeable boundaries) are examined. It is not the intent of this discussion to present test methods designed for determining vertical anisotropy or for determining the location of lateral discontinuities, but rather to examine their effect on constant-rate discharge test response.

4.2.1 Anisotropy

Anisotropy refers to the difference in directional hydraulic conductivity within the tested aquifer. Because of the stratification that is present to some degree in most sediments, vertical anisotropy (K_D) would be expected to influence test results obtained within sedimentary aquifers. In most cases, the vertical hydraulic conductivity within an aquifer is significantly lower than its horizontal counterpart (i.e., $K_v \leq 10^{-1}K_h$).

Low vertical anisotropy ratios accentuate radial flow conditions within the aquifer during testing by decreasing flow in the vertical direction. This is particularly significant for partially penetrating wells. Weeks (1969)

states that vertical anisotropy tends to amplify the drawdown deviations caused by partial penetration within confined aquifers. The amplification of partial penetration effects caused by vertical anisotropy can be used as a means for estimating the K_D . Weeks (1969) presents three methods based on solutions presented in Hantush (1964), which can be used to estimate the vertical anisotropy, provided that the pumping well partially penetrates the aquifer and data for multiple observation wells or piezometers are available. The reader should consult Weeks (1969) for a discussion of each method.

As a simple means of visualizing the effect of vertical anisotropy, Hantush (1964) reports that at a given distance (r) from a partially penetrating stress well, the effects of anisotropy would be the same as those at the distance $r(K_v/K_h)^{1/2}$ within an equivalent isotropic aquifer. The effects of vertical anisotropy, then, can be accounted for in analyzing confined aquifer tests by substituting this relationship for r within equations used for calculating drawdown in confined aquifers [e.g., Equation (3.3)], provided that the ratio of vertical to horizontal conductivity is known or can be estimated independently for the test formation.

For unconfined aquifers, Neuman (1972) reports that where the vertical anisotropy ratio (K_D) is less than 1, the effects of elastic storage and delayed yield (i.e., gravity drainage, as discussed in Section 3.3) are enhanced during the aquifer test. This was shown previously in Figure 3.8, where the lower beta curve values [note Equation (3.17): $\beta = K_D (r^2/b^2)$], lie closely to the early Theis (t_s) elastic response.

For the analysis of anisotropic unconfined aquifer tests, the type-curve procedure should be followed, as outlined previously in Section 3.3.1. The procedure permits the calculation of the vertical anisotropy ratio (K_D) based on Equation (3.17), and the type-curve match beta value. An estimate for K_v can also be obtained if the aquifer thickness is known (note: $K_h = T/b$).

4.2.2 Hydrologic Boundaries

The previous discussions assume that the tested aquifer extends an infinite distance, which allows the area of significant drawdown or "cone of depression" to expand continually with time away from the pumping well during

a constant-rate discharge test. If, during the course of the test, the cone of depression intercepts a hydrologic boundary, i.e., recharge boundary (constant-head) or discharge boundary (no-flow), then drawdown at the pumped well and other points of observation will be affected. For a recharge boundary, drawdown will become constant (i.e., no change with time), while a discharge boundary will cause increased drawdown to occur. On standard log-log plots of pressure drawdown versus time, the presence of boundaries is difficult to discern because the impact of boundaries (unless in close proximity to the pumping well or point of observation) will normally produce a small departure from the homogeneous formation case.

For standard semi-log analysis plots of drawdown versus time, the presence of a recharge boundary eventually produces a horizontal line, while a discharge boundary causes a doubling of slope. While the effects of boundaries are more diagnostic on semi-log plots than on log-log plots because multiple straight-line sections commonly occur, it may be difficult to discern the straight-line section within the drawdown data that actually reflects only test formation properties. As discussed previously in Section 3.0, the section of drawdown data that represents only test formation properties occurs when radial flow conditions have been established during testing and before any boundary effects become significant.

The ambiguity in determining when radial conditions are established and whether a hydrologic boundary has been intercepted during testing is largely removed by using pressure derivatives. As indicated previously in Figure 3.4, hydrologic boundaries exhibit distinct diagnostic pressure derivative patterns. Recharge (i.e., constant head) boundaries are characterized by a pressure derivative pattern that drops steeply towards zero with time, while discharge (i.e., no-flow) boundaries are represented by an initial increase and then stabilization pattern that stabilizes at a derivative value that is double the indicated radial flow condition value (i.e., $p_D' = 1.0$ versus 0.5).

To illustrate the use of pressure derivative analysis for recognizing impermeable boundaries, Figure 4.7 shows the simulated impact of an impermeable boundary on the drawdown response at a fully penetrating pumping well

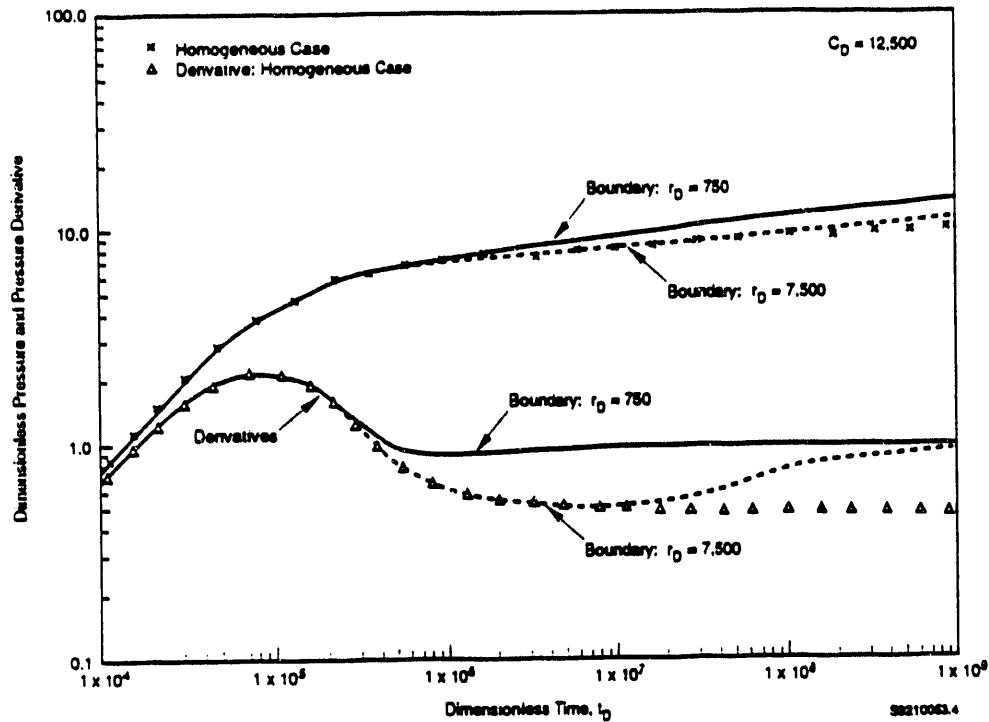


FIGURE 4.7. Effect of an Impermeable Boundary During Constant-Rate Testing for Dimensionless Distances of $r_D = 750$ and 7500

within a confined aquifer. Responses were simulated for impermeable boundaries located at two different dimensionless distances ($r_D = r_o/r_w$) from the pumping well. The figure was developed by superimposing the effect of an image well, which was placed twice the distance from the selected dimensionless radial distances (r_D) of 750 and 7500. The dimensionless pressure response was obtained by summing the effects of the pumping well and the image well, which were calculated individually using a modified version of the TYPCURV program, as originally described in Novakowski (1990). The dimensionless pressure derivative was calculated using the dimensionless pressure data as input to the DERIV program described in Spane and Wurster (1992).

As indicated in Figure 4.7, the diagnostic log-log plot of the pressure derivatives clearly shows the presence of wellbore storage ($C_D = 12,500$) during the early test period (i.e., prior to $t_D = 3 \times 10^5$). This is also indicated by the unit slope on the dimensionless pressure plot. The presence of

the impermeable boundary is not easily recognized on the dimensionless pressure plot, but exhibits a distinct departure on the drawdown derivative beginning at a dimensionless test time of approximately 4×10^5 for a dimensionless boundary distance of 750 and at approximately 2×10^7 for a dimensionless boundary distance of 7500.

Diagnostic log-log analysis of the simulated test examples indicates that radial flow conditions were not attained prior to the establishment of significant boundary effects for the case where the boundary is located at a $r_D = 750$. The use of semi-log, straight-line analysis is, therefore, not valid and the force fitting of a straight line to various sections of the test data would provide inaccurate hydraulic property estimates.

For the test example where the boundary is located at a greater radial distance (i.e., $r_D = 7500$), radial flow conditions were established, starting at a dimensionless test time of approximately 2×10^6 . This is prior to the time that significant boundary effects are manifest. Semi-log, straight-line analysis of the delineated radial flow region (i.e., $t_D =$ from 2×10^6 to 2×10^7) is therefore valid and will provide an accurate estimate of the test formation hydraulic properties.

4.3 EXTERNAL STRESS FACTORS

External aquifer stress factors can adversely affect the conduct and analysis of constant-rate discharge tests. Conditions that increase the influence of external stress factors are tests conducted at low stress (i.e., drawdown) levels, tests conducted in aquifers possessing high transmissivities, wells located in close proximity to fluctuating surface-water bodies (i.e., rivers), and aquifers having high rigidity (i.e., high compressive strength). In this section, external stress factors that are relatively systematic will be examined, such as barometric and river-stage fluctuations. Other systematic stresses such as ocean tide and earth tide variations are not discussed. Corrections for these factors, however, would be similar to those discussed for barometric and river-stage effects.

4.3.1 Barometric Fluctuation

Barometric fluctuation effects refer to the change in formation pressure associated with changes in atmospheric pressure. Although barometric fluctuations represent an areal, blanket stress applied to the aquifer, the magnitude of formation pressure change at any particular locality is a function of the degree of aquifer confinement, rigidity of the aquifer matrix, and the specific weight of ground water.

For constant-rate tests conducted in semi-confined to confined aquifers, hydraulic test results can be corrected for the effects of barometric fluctuations using the method described by Clark (1967) for determination of barometric efficiency. The removal of barometric effects would be expected to be most important for hydraulic tests of long duration (e.g., pumping tests) and/or tests with expected low hydraulic responses (e.g., slug interference tests). Briefly stated, the removal of barometric fluctuations requires the following steps:

1. collection of test site atmospheric pressure values and associated aquifer formation pressure values for a pre- or post-test period, during which no other extraneous stresses are imposed on the aquifer
2. determination of the barometric efficiency (BE) for each well site following the procedure outlined in Clark (1967)
3. removal of barometric induced changes from the measured test response.

The barometric efficiency of an open well/aquifer system was first defined by Jacob (1940) as:

$$BE = -\bar{\tau}_{fc} (\Delta h_s / \Delta P_o) \quad (4.2)$$

where $\bar{\tau}_{fc}$ = average specific weight of the fluid column in the well [F/L³]

Δh_s = change in elevation of the fluid column in the well associated with atmospheric pressure change [L]

ΔP_o = change in atmospheric pressure [F/L²].

Downhole pressure measured within an open well is in equilibrium with the pressure in the aquifer (P_f) at the measurement elevation point. This pressure responds immediately to atmospheric pressure fluctuations, but at a magnitude equal to the atmospheric pressure change minus the pressure change caused by the change in the fluid column elevation within the well (Spaine and Mercer 1985):

$$\Delta P_f = \Delta P_o + \bar{\tau}_{fc} \Delta h_s \quad (4.3)$$

or combining with Equation (4.2)

$$\Delta P_f = (1-BE) \Delta P_o \quad (4.4)$$

Equations (4.3) and (4.4) indicate that the change in downhole formation pressure represents only that portion of the atmospheric pressure change not borne by the test formation matrix. Therefore, high barometric efficiencies reflect high strength and rigid test formations, while low efficiencies indicate highly compressible formations.

The Clark method is particularly applicable in calculating barometric efficiencies from test interval responses that are influenced by other extraneous pressure trends. Briefly stated, the method determines the barometric efficiency from the slope of a summation plot of the incremental changes in downhole formation pressure, $\Sigma \Delta P_f$, versus the incremental change in atmospheric pressure, $\Sigma \Delta P_o$. Incremental changes in downhole formation pressure are added to the summation total when the incremental sign change is equal to that of the incremental atmospheric pressure (ΔP_o) sign change for the observed incremental period (e.g., when ΔP_f and ΔP_o are both positive or negative). Conversely, incremental changes in downhole formation pressure are subtracted from the summation total when the incremental sign change is unequal to that of the incremental atmospheric pressure sign change for the observed period. In addition, no incremental change in downhole formation pressure is added to the summation total when no change in atmospheric pressure is recorded.

Once the barometric efficiency value is determined for an individual well, the effects of barometric pressure change during the course of the test can be corrected by removing the associated calculated water-level or formation pressure response from the test record using Equations (4.2), (4.3), or (4.4) and solving for either Δh_s or ΔP_f . An example of the beneficial removal of barometric pressure effects from low-level stress slug interference tests conducted on the Hanford Site is provided in Spane (1992a).

4.3.2 River-Stage Fluctuation

River-stage fluctuation effects refer to changes in formation pressure associated with changes in nearby river-stage elevation. Unlike barometric fluctuations, the stress effects of river-stage fluctuations are not spatially uniform or applied instantaneously to the entire aquifer. As discussed in Ferris et al. (1962), the magnitude of formation pressure change at any particular locality is primarily a function of the distance from the river, the hydraulic diffusivity of the intervening aquifer materials (i.e., from the point of observation to the river), and the nature of the aquifer contact with the river (i.e., direct hydraulic communication or loading model).

At the Hanford Site, it has been noted previously that Columbia River-stage fluctuations exert a discernible effect on water-level responses within the unconfined aquifer for distances up to approximately 1 1/2 to 2 miles from the river on the Hanford Site (Newcomb et al. 1972). A number of recent studies have examined the magnitude of well responses and time lags associated with river-stage fluctuations on the Hanford Site (e.g., Gilmore et al. 1990, 1992).

The effects of river-stage fluctuation can be removed using the procedure previously outlined for removing barometric fluctuation. The well data records must first be shifted to account for the time-lag exhibited between the well water-level data and river-stage fluctuations. A description of the statistical procedure used in determining the time-lag for a well is provided in Gilmore et al. (1992). For the removal of river-stage effects, the apparent tidal efficiency (TE_a) is calculated for each well by replacing the BE in Equations (4.2) and (4.4) with TE_a . As for barometric fluctuations, river-stage effects are expected to be more important for hydraulic tests of long

duration (e.g., pumping tests) and/or tests with expected low hydraulic responses (e.g., slug interference tests). These effects, however, would only be observed at test sites located within several miles from the river.

4.3.3 Extraneous Stress Removal

To demonstrate the removal of barometric pressure and river-stage effects from well water-level records, data obtained during June 1992 at well 699-15-E13 (DB-2) on the Hanford Site were examined. Well DB-2 is completed in a confined aquifer and located approximately 0.5 miles from the Columbia River. Figure 4.8(a) presents the visual correlation of river-stage fluctuation and water-level responses within well DB-2. Note that the well water-level scale used in the figure is exaggerated by a factor of 3 (i.e., 1 m versus 3 m) in comparison to the river stage, to enhance the visual correlation. The apparent tidal efficiency (TE_a) from the well hydrograph record was calculated following the procedure outlined in Section 4.3.2, and the river-stage effects were removed, based on the calculated apparent tidal efficiency and the observed river-stage elevations.

Figure 4.8(b) shows the correlation of atmospheric pressure readings (as recorded at the Hanford Meteorological Station) and well DB-2 water levels that have been corrected for river-stage fluctuations. As shown, a clear association with atmospheric pressure readings is indicated within the corrected well hydrograph record. This association is, however, not readily apparent in the uncorrected well record (Figure 4.8a) due to the significant effect of river-stage fluctuations.

The BE for well DB-2 was calculated following the procedure outlined in Section 4.3.1, and the effects of barometric pressure fluctuations were removed from well DB-2 water-level data based on the calculated BE and the observed barometric pressure record. Figure 4.9 shows the comparison of the uncorrected and totally corrected (i.e., for river-stage and atmospheric pressure fluctuations) water-level record at well DB-2. As indicated, extraneous stress effects have been effectively removed.

The results of this test example demonstrate that the effects of extraneous stresses can be removed from constant-rate discharge test data records

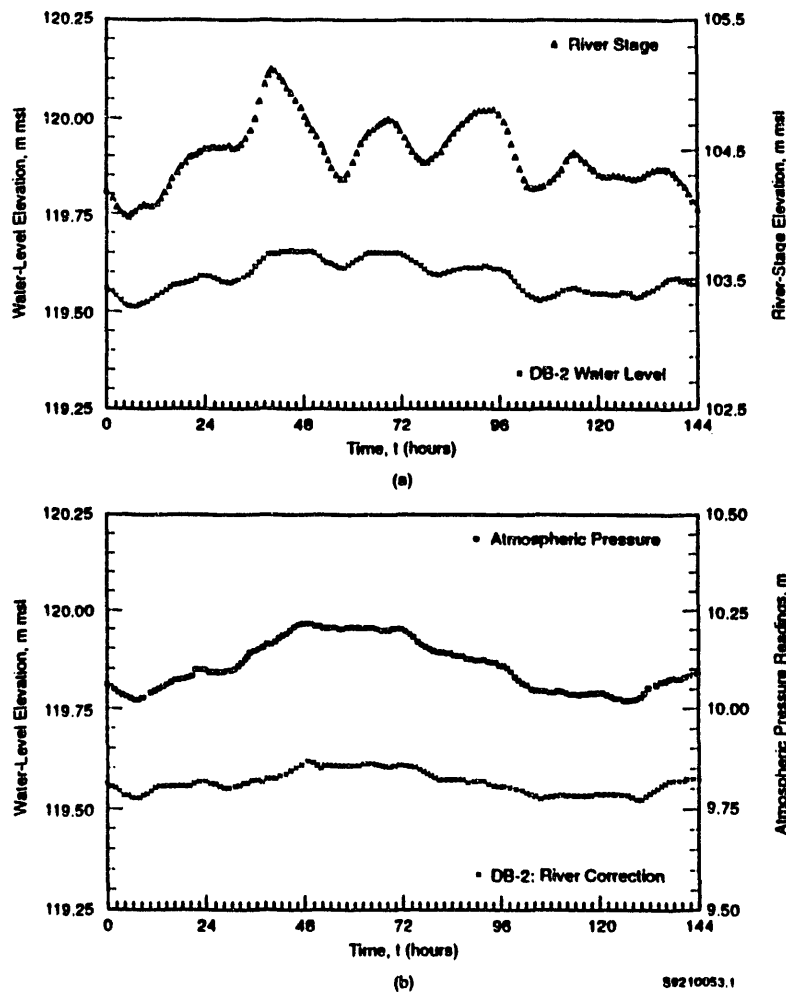
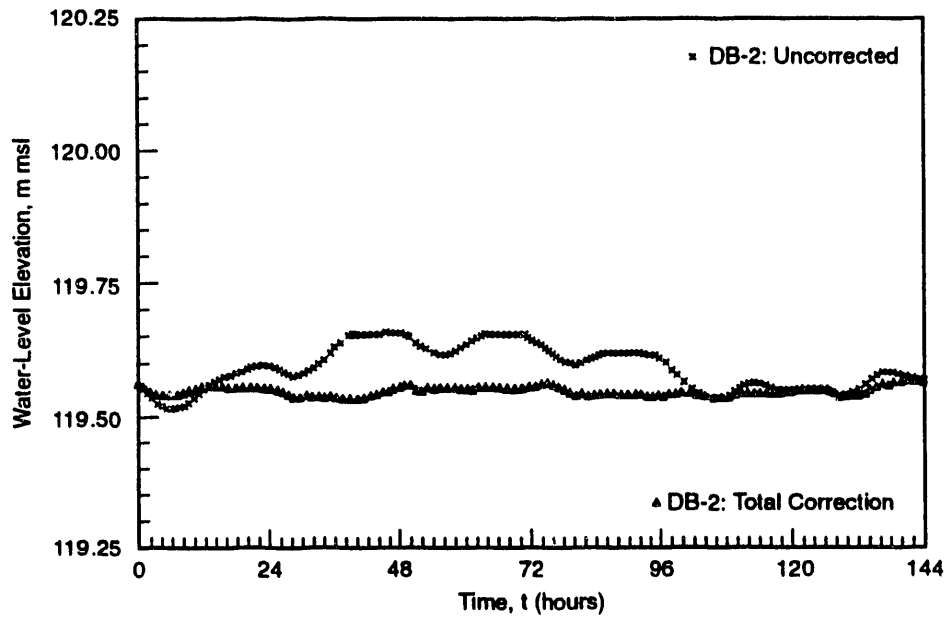


FIGURE 4.8. Example of External Stress Factor Removal for Well DB-2: (a) Comparison of Uncorrected DB-2 Water Levels and Columbia River-Stage Fluctuations and (b) Comparison of River-Stage Corrected DB-2 Water Levels and Atmospheric Pressure Variations

This is particularly important for tests conducted at sites located in close proximity to the river (i.e., up to several miles away), for aquifers possessing high transmissivities and/or for tests that impose only small hydraulic stresses on the test formation. It should also be noted that the extraneous stress removal techniques demonstrated in Figures 4.8 and 4.9 can be used



S9210053.2

FIGURE 4.9. Comparison of Uncorrected Well DB-2 Water Levels and Fully Corrected Well DB-2 Water Levels with Extraneous Stress Effects Removed

directly in estimating areal hydraulic diffusivity surrounding the monitored well (see Jacob 1950; Ferris 1962; Gilmore et al. 1992 for a discussion of these analysis techniques).

5.0 TEST DATA ANALYSIS

Results from three constant-rate test examples are provided to demonstrate the analysis procedures and use of pressure derivatives discussed in this report. The three constant-rate tests are taken from well-known test examples previously reported in the literature. The tests examined include two confined aquifer and one unconfined aquifer test.

The general analysis procedure includes construction of an initial, diagnostic log-log drawdown and drawdown derivative plot for the purpose of identifying aquifer response characteristics (i.e., homogeneous versus heterogeneous formation response) and for identifying the establishment of radial flow regions within the test data. The identified radial flow region is then analyzed using semi-log, straight-line analysis methods. After semi-log, straight-line analysis is completed, additional corroboration in hydraulic property estimates is obtained through appropriate type-curve matching solutions, i.e., nonleaky confined aquifer (Theis 1935), leaky confined aquifer (Hantush and Jacob 1955; Hantush 1960), and unconfined aquifer (Neuman 1975).

5.1 CONFINED AQUIFER EXAMPLES

Two test examples are provided that illustrate the analysis of nonleaky confined aquifer tests and the analysis of leaky confined aquifer tests with confining layer storage.

5.1.1 Nonleaky Test Example

For this test example, time/drawdown data from a fully penetrating observation well were examined for a constant-rate discharge test conducted within an infinite, nonleaky confined aquifer. The test example is presented to demonstrate the determination of radial flow conditions within a test data set that displays test "noise" typically encountered in many field test situations. The observation well test data are for Well 1, Gridley, Illinois, as listed in Walton (1962 and 1987). Pertinent test information includes:

discharge rate = 832.8 L/min (220 gpm)

distance from pumping well = 251.2 m (824 ft)

and reported analysis results are:

transmissivity = 125.4 m²/d (1350 ft²/d)

storativity = 2 x 10⁻⁵.

Figure 5.1 shows the diagnostic log-log plot of the drawdown and drawdown derivative calculated using the DERIV program (Spang and Wurster 1992). The figure indicates that radial flow conditions were established after a test time of approximately 70 min. Figure 5.2 shows the semi-log, straight-line analysis for data in the identified radial flow section of the test (i.e., $t > 70$ min), which yields hydraulic property estimates of transmissivity = 128.8 m²/d, and storativity = 1.83 x 10⁻⁵. This compares favorably with the

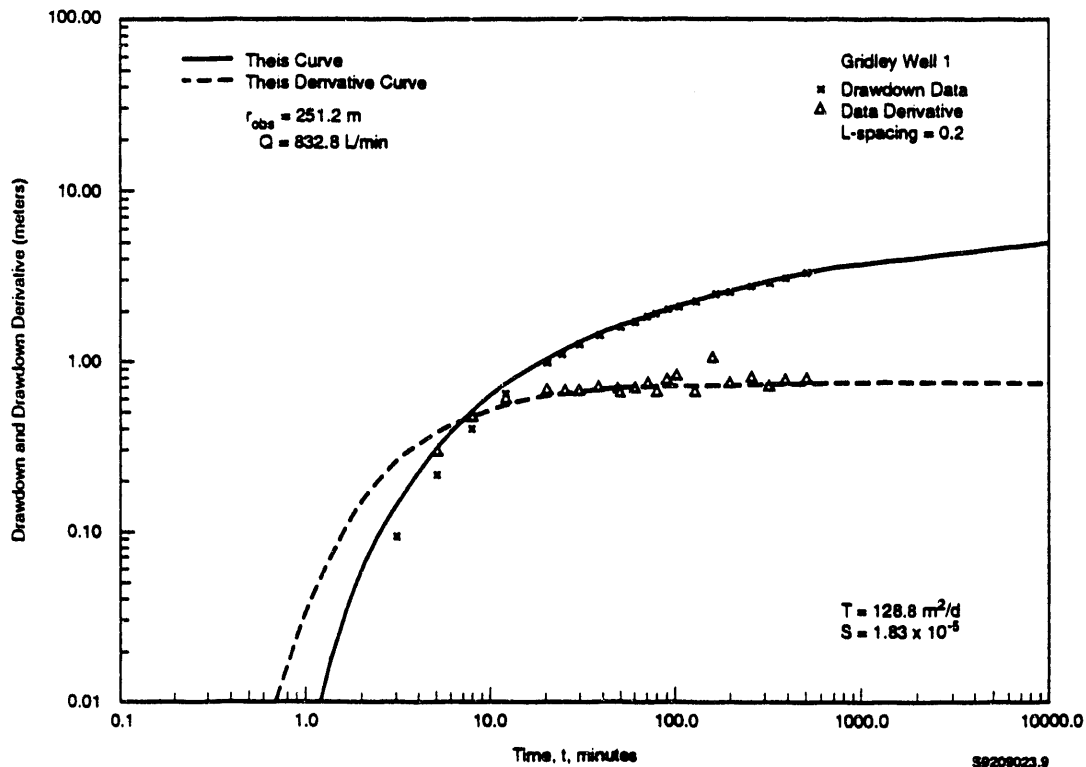


FIGURE 5.1. Diagnostic Log-Log Analysis Plot and Type Curve Match for Nonleaky Confined Aquifer Test Example (Gridley Well 1, Illinois)

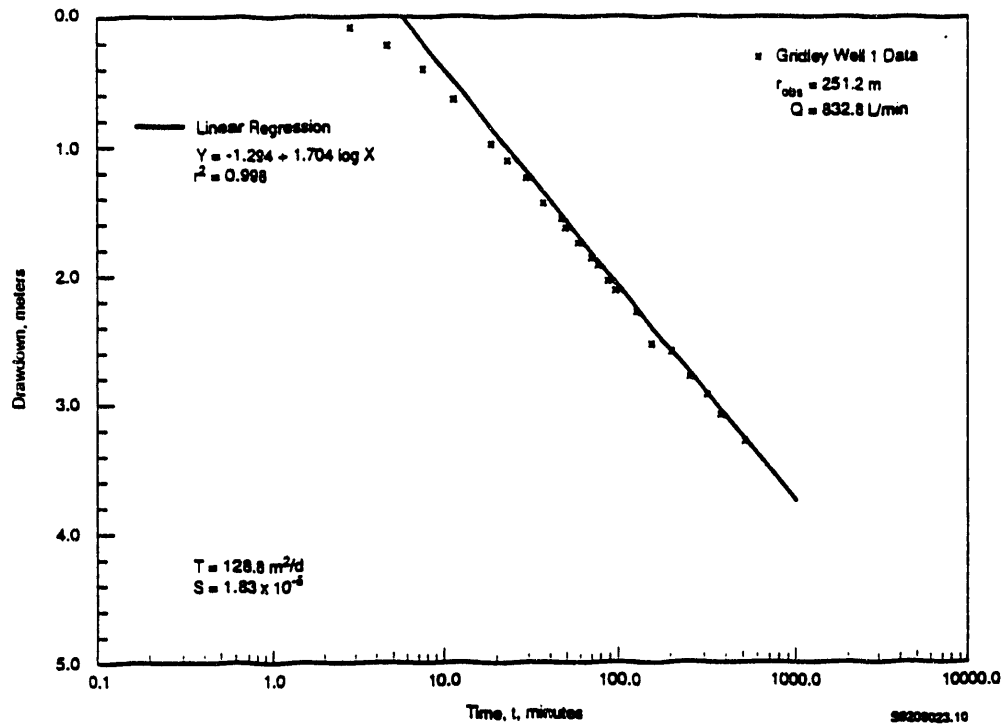


FIGURE 5.2. Semi-Log, Straight-Line Analysis for Nonleaky Confined Aquifer Test Example (Gridley Well 1, Illinois)

previously reported values. For corroboration, the Theis curve and Theis derivative curve responses for these hydraulic property and distance relationships are shown superimposed on the test data in Figure 5.1. As indicated, a good match between test data and type curves was obtained.

5.1.2 Leaky Test Example

For this test example, time/drawdown data from a fully penetrating observation well were examined for a constant-rate discharge test conducted within an infinite, leaky confined aquifer with significant confining layer storage. The test example is presented to demonstrate the use of pressure derivatives in selecting the correct leaky aquifer with confining layer storage type curve (i.e., $H(u,B)$ type curves presented in Hantush 1960, 1964) for test analysis. As indicated in Luhman (1972), "...thorough knowledge of the

geology, including the character of the confining beds should indicate in advance which of the two leaky-aquifer type curves to use, or whether to use the Theis type curve for nonleaky aquifers."

As indicated in Section 3.2, the pressure derivatives for the two types of leaky aquifer conditions display significantly different patterns, and therefore, should be readily distinguished by diagnostic log-log analysis. The difference between some of the leaky aquifer (with storage) pressure derivative type curves and the nonleaky (i.e., Theis) derivative type curve may be less obvious. However, when combined with pressure drawdown type curves, the pressure derivative curves provide a means of distinguishing the correct leaky aquifer type-curve match. This is because of differences in the intersection relationships for the corresponding pressure drawdown and draw-down derivatives.

For this test example, observation well test data are analyzed for Well 23S/25E-17Q2, at Pixley, California, as listed in Lohman (1972). Pertinent test information includes:

discharge rate = 2839.1 L/min (750 gpm)

distance from pumping well = 426.7 m (1400 ft)

and reported analysis results are:

transmissivity = 201.6 m²/d (2170 ft²/d)

storativity = 3.9 x 10⁻⁵

Figure 5.3 shows the diagnostic log-log plot of the drawdown and draw-down derivative calculated using the DERIV program (Spane and Wurstner 1992). The figure indicates a pattern that "resembles" a Theis derivative curve in general appearance. When combined with pressure drawdown data, however, the drawdown data and data derivative curves display a diagnostic pattern that cannot be matched with a combined Theis and Theis derivative type curve. Lohman (1972) states that attempts to force fit either early- or late-time data with the Theis curve gave estimates for transmissivity that ranged between 5 to 20 times the cited correct value (i.e., 200 m²/d), and apparent values for storativity from 17 to 25 times those reported for the aquifer.

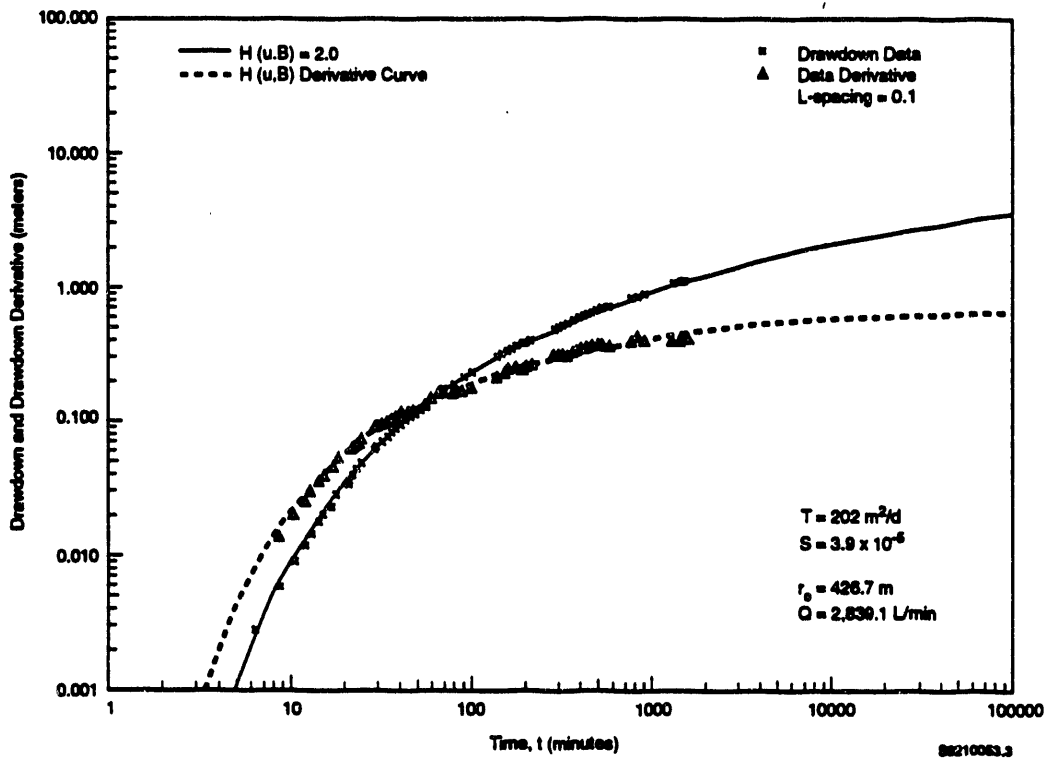


FIGURE 5.3. Diagnostic Log-Log Analysis Plot and Type Curve Match for Leaky Confined Aquifer Test Example (Pixley Well, California)

Because the test data and data derivative plots do not indicate infinite-acting, radial flow conditions, semi-log, straight-line analysis is not possible for this test example. To facilitate the analysis of the test data, derivative type curves were calculated from type curves listed for selected B values (e.g., Hantush 1964) using the DERIV program (see Figure 3.6). The test data and data derivatives were then matched with the log-log dimensionless drawdown and dimensionless derivative curves. As indicated in Figure 5.3, the drawdown data and data derivatives are closely matched over their entirety, with a leaky aquifer type curve having a B value of 2.0. This type-curve match provides estimates for transmissivity and storativity that are identical with those reported in Lohman (1972), i.e., $202 \text{ m}^2/\text{d}$ and 3.9×10^{-5} , respectively.

5.2 UNCONFINED AQUIFER EXAMPLE

For this test example, time/drawdown data from a fully penetrating observation well were examined for the unconfined aquifer test conducted at the Fairborn Well in Dayton, Ohio, as listed in Lohman (1972). The test example is presented to demonstrate the use of both confined and unconfined aquifer solution methods that were presented previously in Section 3.3 for analyzing unconfined aquifer tests.

The general analysis procedure for the unconfined aquifer test example includes an initial, diagnostic log-log drawdown and drawdown derivative plot for identifying aquifer response characteristics (i.e., homogeneous versus heterogeneous formation response) and for identifying the establishment of radial flow regions. Identified radial flow regions can then be analyzed using semi-log, straight-line confined aquifer analysis methods. After completion of the analysis based on the confined aquifer solution, an additional type-curve matching analysis, based on unconfined aquifer solutions (Neuman 1975) is presented.

Pertinent test information includes:

observation well distance = 22.25 m (73 ft)

aquifer thickness = 23.77 m (78 ft)

constant-rate discharge = 4088.2 L/min (1080 gpm)

and reported analysis results are:

transmissivity = 3250 m²/d (35,000 ft²/d)

storativity = 3×10^{-3}

specific yield = 0.09

5.2.1 Analysis Using the Confined Aquifer Solution

This test analysis example is presented to demonstrate the use of pressure derivatives in determining when radial flow conditions are established, and therefore, when confined aquifer (i.e., nonleaky) analysis procedures are applicable for analyzing unconfined aquifer tests.

As was discussed in Section 3.0, constant-rate discharge tests conducted within fully penetrating wells in unconfined aquifers are characterized by the presence of three distinct segments on a time-drawdown curve. The first and third segments follow the drawdown response as predicted by the Theis solution, with aquifer storage equal to its storativity for the first flow segment, and aquifer storage equal to the sum of its storativity and specific yield for the third flow segment.

Diagnostic log-log analysis of unconfined aquifer tests can be used to identify the existence of unconfined aquifer delayed-yield response and whether radial flow conditions have been established during the first or third segments of the unconfined aquifer curve, thereby verifying the applicability of confined aquifer analysis for these test data segments.

Figure 5.4 shows the diagnostic log-log plot of the test example drawdown data, which exhibits a number of characteristic features. The drawdown data plot displays a classic "three-segment" unconfined aquifer response. The first segment follows an early Theisian type of response (elastic response = S). This is followed by an essentially horizontal second segment indicative of delayed-yield. The third segment conforms to a non-elastic, late-Theisian response (non-elastic = $S_y + S$, where $S_y \gg S$).

The drawdown derivative plot shown in the figure also displays distinct patterns for the unconfined aquifer response. The derivative plot indicates the following:

1. Radial flow conditions were not fully reached during the "first segment" of the test response (i.e., < 1 min); therefore, semi-log, straight-line analysis of this data segment is not valid.
2. The delayed-yield segment is indicated by the decline in the drawdown derivative that begins at a test time of approximately 1 min.
3. Radial flow conditions during the third segment are indicated by the stabilized drawdown derivative after a test time of 500 min. Semi-log, straight-line analysis of test data during this region is therefore valid.

Figure 5.5 shows the semi-log, straight-line analysis of the radial flow segment of the test data (i.e., $t > 500$ min), which yields hydraulic property

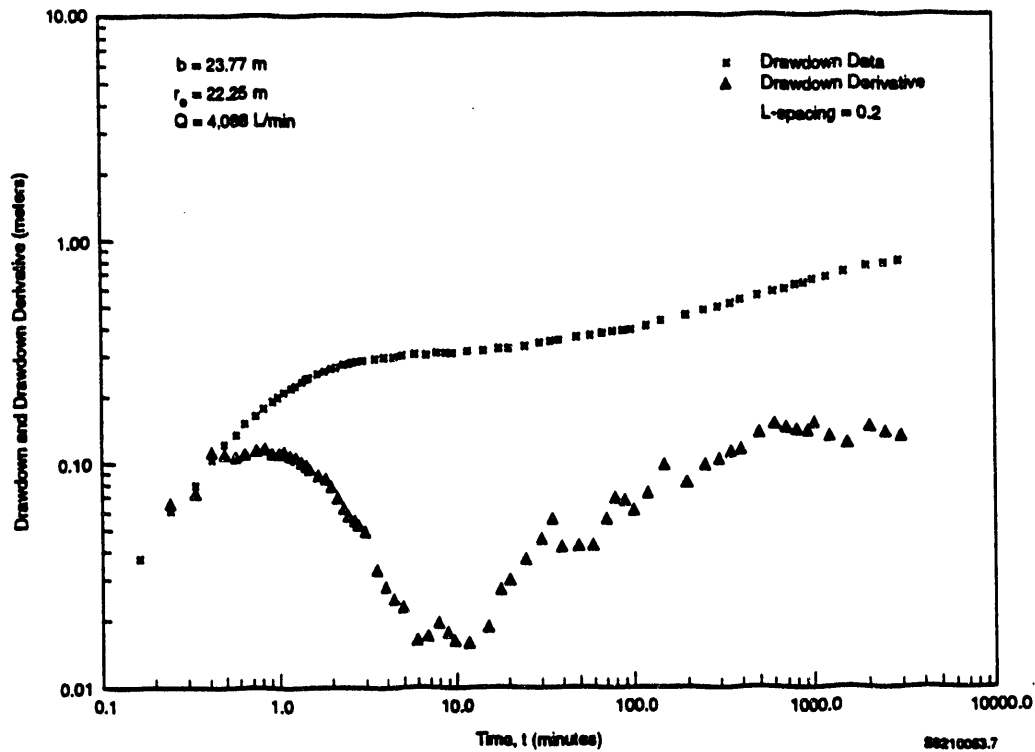


FIGURE 5.4. Diagnostic Log-Log Analysis Plot for Unconfined Aquifer Test Example (Fairborn Well, Dayton, Ohio)

estimates of transmissivity = $3435 \text{ m}^2/\text{d}$ and specific yield = 0.083. This compares favorably with the previously reported values. For corroboration, the Theis curve and Theis derivative curve responses for these hydraulic property and distance relationships are shown superimposed on the drawdown data in Figure 5.6. As indicated, a good match between test data and type curves was obtained. It should be noted that the early-time Theis curve match was obtained by using a storativity of 0.003, as reported in Lohman (1972).

5.2.2 Unconfined Aquifer - Type-Curve Analysis

In addition to the analysis based on the confined aquifer solution, type-curve matching analysis based on unconfined aquifer solution type curves (Neuman 1975) can also be performed on the test drawdown data. Because all three segments of unconfined aquifer flow were exhibited in Figure 5.4, Neuman

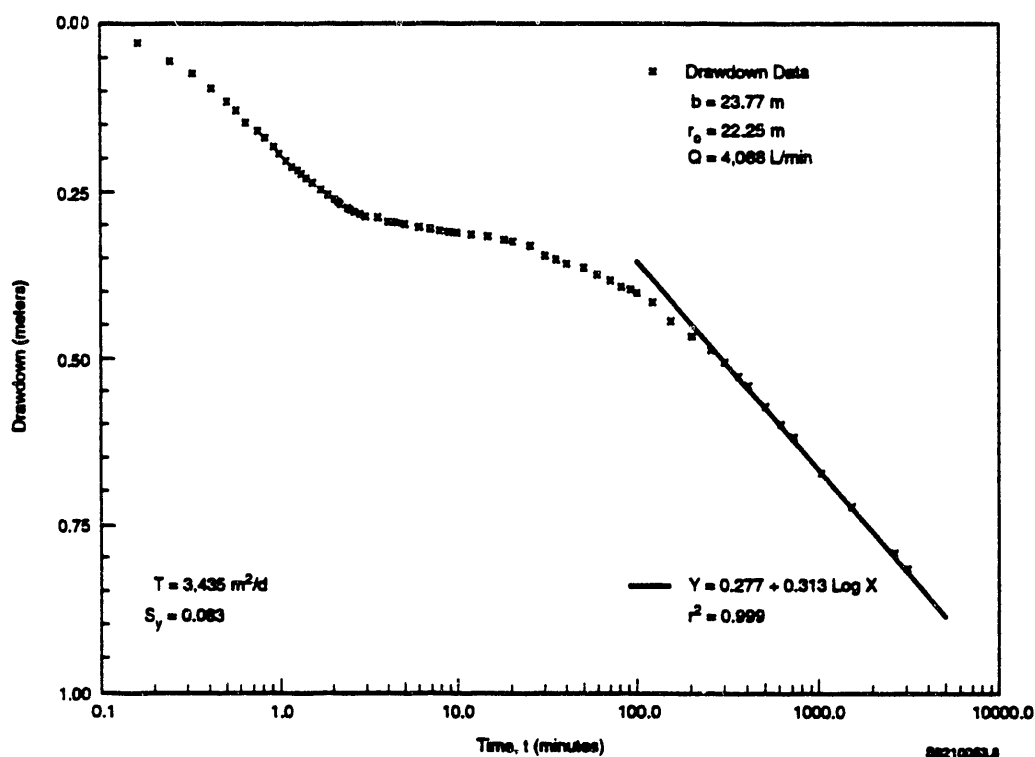


FIGURE 5.5. Semi-Log, Straight-Line Analysis for Unconfined Aquifer Test Example (Fairborn Well, Dayton, Ohio)

type A curves (for analysis of segments 1 and 2) and type B curves (for analysis of segments 2 and 3) can be used. The general analysis procedure includes:

- plotting the drawdown data and drawdown data derivatives for segments 1 and 2, and 2 and 3
- matching the test data and data derivatives with the appropriate type A and type B curves, respectively
- calculating the hydraulic properties based on the match points and match curve used in the analysis.

Type A Curve Analysis

Figure 5.7 shows the type-curve match for segments 1 and 2 of the test data, with the final match curve corresponding to a β value of 0.20. The final β curve match was selected by visual curve matching of the test data and data derivative. While other β type curves could be used to match the

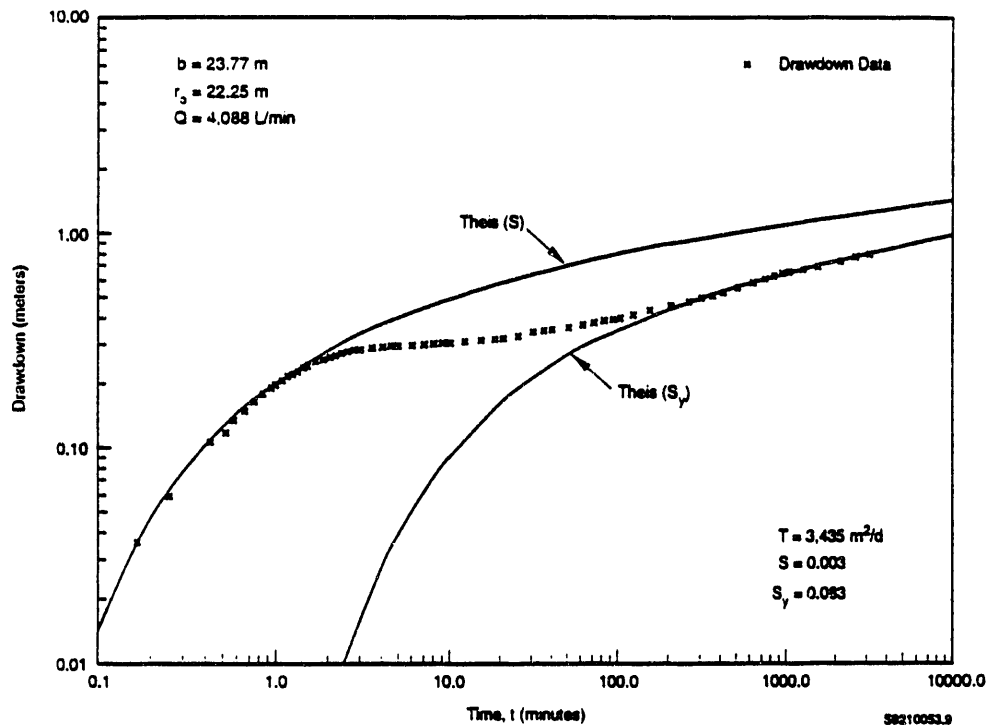


FIGURE 5.6. Confined Aquifer Type Curve (Theis Curve) Analysis for Unconfined Aquifer Test Example (Fairborn Well, Dayton, Ohio)

drawdown data plot (because of their similar shape - see Section 3.3.1), the simultaneous matching of the data derivative with the type-curve derivative provided the basis for selecting the $\beta = 0.20$ curve. The type curves were generated with the DELAY2 program, which was originally described in Neuman (1975), although type-curve matching with existing published curves could also have been used. The derivatives for the type curves were calculated using the DERIV program (Spang and Wurster 1992).

As indicated in Figure 5.7, a good drawdown data and data derivative match was obtained using a beta value of 0.20. Based on the curve-match analysis, the following match points were obtained: $t = 0.96$ min, $t_s = 1.0$, $s = 0.277$ m, and $s_D = 1.0$. Following the analysis procedure outlined in Section 3.3.1, the match-point values provide estimates of transmissivity and storativity of $1690 \text{ m}^2/\text{d}$ and 0.002, respectively. The storativity estimate

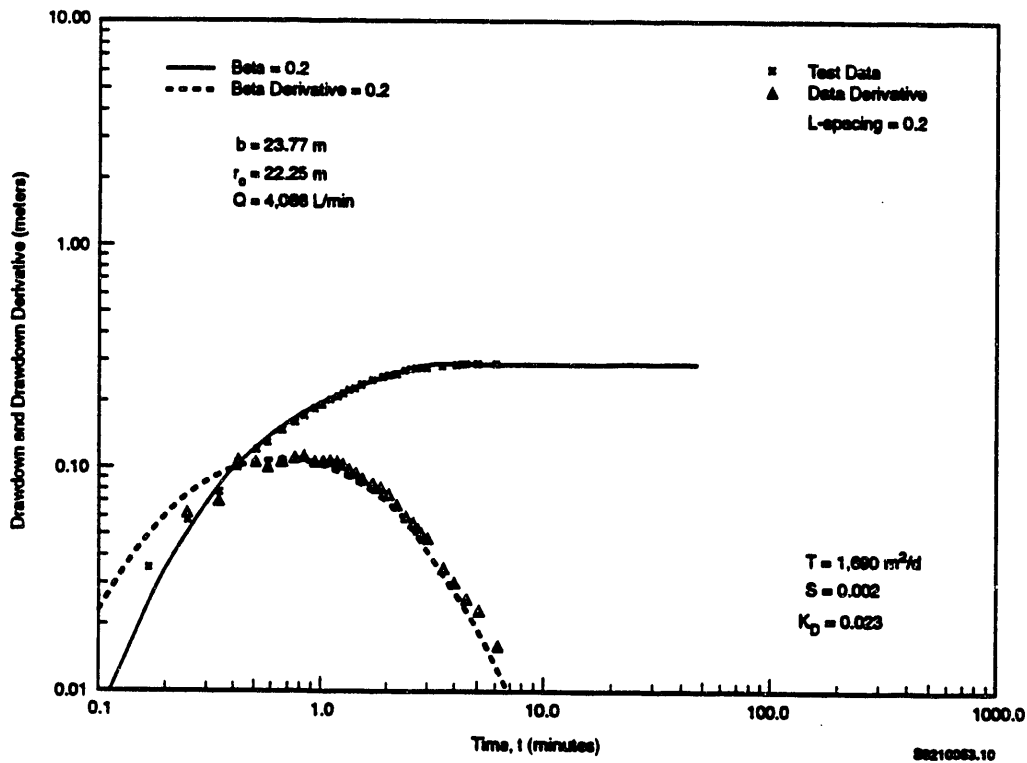


FIGURE 5.7. Unconfined Aquifer Type A Curve and Derivative Analysis for Unconfined Aquifer Test Example (Fairborn Well, Dayton, Ohio)

is close to the value of 0.003) reported in Lohman (1972); however, the estimate for transmissivity is lower by a factor of two (1690 versus 3250 m²/d). The reason for the difference in transmissivity estimates is not readily apparent. Type A curve analysis is dependent on the analysis of the initial test responses, which can be adversely affected by nonformational effects previously discussed (e.g., wellbore storage effects) and nonuniform discharge rates that are common during the early stages of constant-rate testing. For these reasons, and due to the similarity in the type A curve shapes, superior analytical results are expected from type B curve matching.

Type B Curve Analysis

Figure 5.8 shows the type-curve match for segments 2 and 3 of the test data, with the final match curve corresponding to a β value of 0.04. The final β curve match was selected by visual curve matching of the test data and data derivative. As in the type A curve analysis, the type curves and

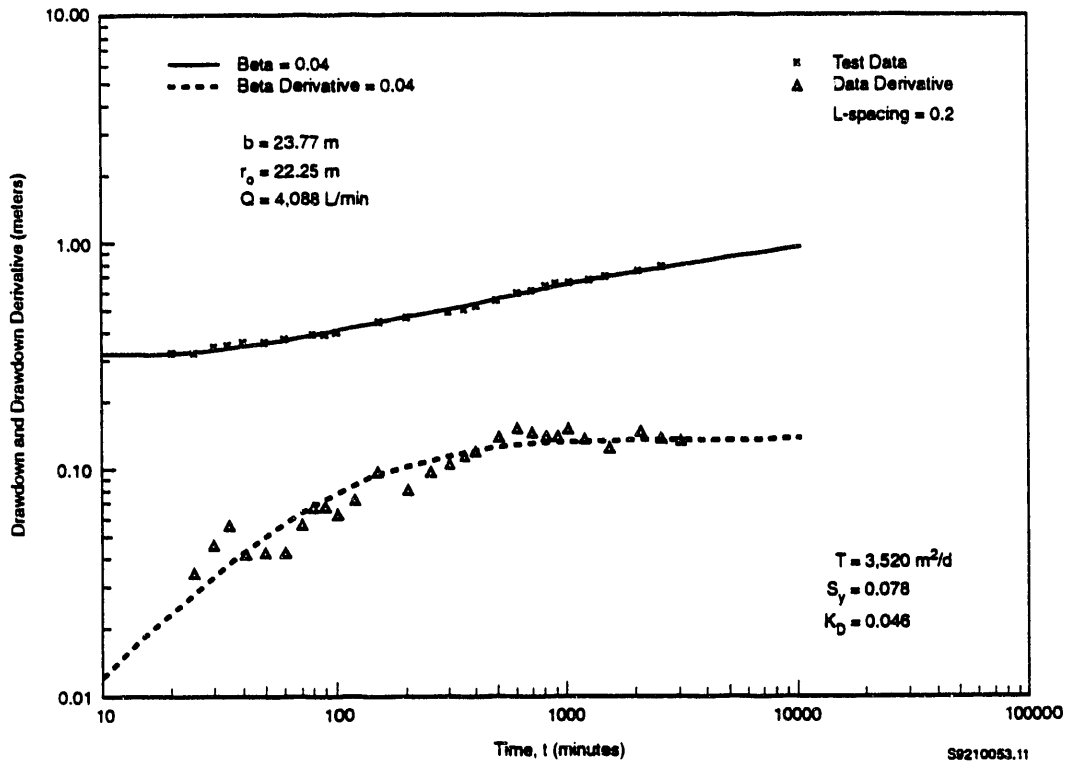


FIGURE 5.8. Unconfined Aquifer Type B Curve and Derivative Analysis for Unconfined Aquifer Test Example (Fairborn Well, Dayton, Ohio)

derivatives were generated with the DELAY2 and DERIV programs, respectively. Unlike type A curve analysis, type B type curves display significant differences in shape, especially for β values greater than 0.01 (see Figure 3.10). In addition, the type B derivative patterns are more unique because the derivatives merge with time to form a horizontal line. The fact that the type B derivatives form a horizontal line reduces the ambiguity of the overall type-curve match because the vertical axis of the match is fixed by the horizontal derivative line.

As indicated in Figure 5.8, a good match to the drawdown data and data derivative was obtained using a β value of 0.04. Based on the curve-match analysis, the following match points were obtained: $t = 15.8$ min, $t_y = 1.0$, $s = 0.133$ m, and $s_D = 1.0$. Following the analysis procedure outlined in Section 3.3.1, the match-point values provide estimates of transmissivity and specific yield of $3520 \text{ m}^2/\text{d}$ and 0.078, respectively. The transmissivity and

specific yield estimates are in close agreement with the values (i.e., $T = 3250 \text{ m}^2/\text{d}$; $S_y = 0.09$) reported in Lohman (1972) and values obtained from the confined aquifer analysis reported in Section 5.2.1 (i.e., $T = 3435 \text{ m}^2/\text{d}$; $S_y = 0.083$). Based on the calculated value for transmissivity of $3520 \text{ m}^2/\text{d}$, an aquifer thickness of 23.77 m, and a β value of 0.04, Equation (3.17) can be used to provide an estimate for vertical hydraulic conductivity for the aquifer of 5.2 m/d and a vertical anisotropy value (i.e., K_v/K_h) of 0.035. The vertical anisotropy value also compares favorably with the estimate of 0.027 reported in Lohman (1972).

Complete Unconfined Curve Analysis

Figure 5.9 shows the type-curve match analysis for segments 1, 2, and 3 of the test data, based on results obtained from the type B curve analysis (i.e., β curve = 0.04; $T = 3520 \text{ m}^2/\text{d}$; $S_y = 0.078$). A slightly better match was obtained using the storativity value (0.003) reported in Lohman (1972),

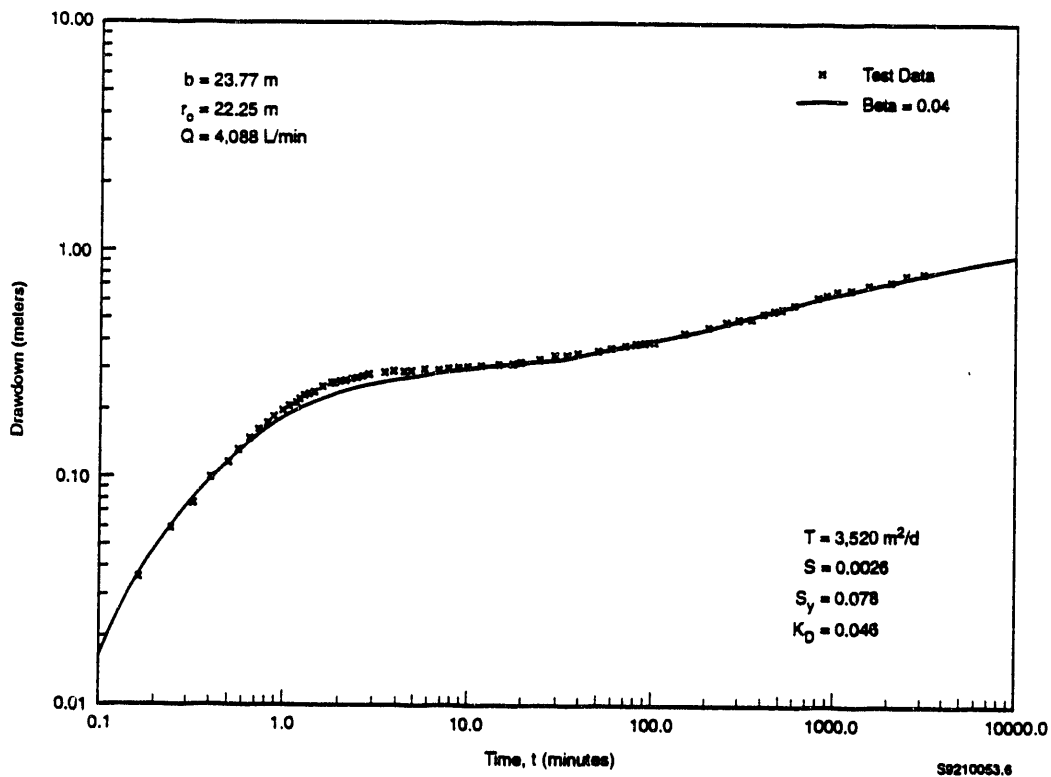


FIGURE 5.9. Complete Unconfined Aquifer Type Curve Analysis for Unconfined Aquifer Test Example (Fairborn Well, Dayton, Ohio)

rather than the estimate (0.002) obtained from the type A curve analysis. As in the previous type A and B curve analyses, the type curves and derivatives were generated with the DELAY2 and DERIV programs, respectively.

As indicated in Figure 5.9, close agreement in predicted and observed response was obtained for most of the test. The only significant area of departure occurred during part of the early stages of the test (between 0.75 and 4 min). The reason for this observed departure is not completely understood; however, it may be related to factors previously discussed that affect early-time constant-rate tests (e.g., wellbore storage or variations in discharge rate).

6.0 REFERENCES

- Agarwal, R. G., R. Al-Hussainy, and H. J. Ramey, Jr. 1969. "An Investigation of Wellbore Storage and Skin Effect in Unsteady Liquid Flow." Soc. of Petrol. Eng. J. 10(3).
- Agarwal, R. G. 1980. "A New Method to Account for Producing Time Effects when Drawdown Type Curves are Used to Analyze Pressure Buildup and Other Test Data." Presented at the 1980 Society of Petroleum Engineers Annual Technical Conference and Exhibition, Sept. 21-24, 1980, Dallas. SPE Paper 9289.
- Beauheim, R. L., and J. F. Pickens. 1986. "Applicability of the Pressure Derivative to Hydraulic Test Analysis." Presented at the Annual Meeting of the American Geophysical Union, May 19-22, 1986. Baltimore, Maryland.
- Boulton, N. S. 1954. "The Drawdown of the Water-Table Under Non-Steady Conditions Near a Pumped Well in an Unconfined Formation." In Proceedings, Institute of Civil Engineers, vol. 3, Part 3, pp. 564-579.
- Boulton, N. S. 1963. "Analysis of Data from Nonequilibrium Pumping Tests Allowing for Delayed Yield from Storage." In Proceedings, Institute of Civil Engineers, vol. 26, pp. 469-482.
- Bourdet, D., T. M. Whittle, A. A. Douglas, and Y. M. Pirard. 1983a. "A New Set of Type Curves Simplifies Well Test Analysis." World Oil, May 1983, pp. 95-106.
- Bourdet, D., J. A. Ayoub, T. M. Whittle, Y. M. Pirard, and V. Kniazeff. 1983b. "Interpreting Well Tests in Fractured Reservoirs." World Oil, October 1983, pp. 77-87.
- Bourdet, D. A. Alagoa, J. A. Ayoub, and Y. M. Pirard. 1984. "New Method Enhances Well Test Interpretations." World Oil, September 1984, pp. 37-44.
- Bourdet, D., J. A. Ayoub, and Y. M. Pirard. 1989. "Use of Pressure Derivative in Well-Test Interpretation." Society of Petroleum Engineers, SPE Formation Evaluation, June 1989, pp. 293-302.
- Chapuis, R. P. 1992. "Using Cooper-Jacob Approximation to Take Account of Pumping Well Pipe Storage Effects in Early Drawdown Data of a Confined Aquifer." Ground Water 30(3):331-337.
- Clark, W. E. 1967. "Computing the Barometric Efficiency of a Well." In Proceedings of the American Society of Civil Engineers, Journal of the Hydraulics Division 43(HY4):93-98.
- Cooper, H. H., Jr., and C. E. Jacob. 1946. "A Generalized Graphical Method for Evaluating Formation Constants and Summarizing Well-Field History." American Geophysical Union, Transactions 27(4):526-534.

- Dagan, G. 1967. "A Method of Determining the Permeability and Effective Porosity of Unconfined Anisotropic Aquifers." Water Resour. Res. 3(4).
- Earlougher, R. C., Jr. 1977. Advances in Well Test Analysis. Soc. of Petroleum Engineers, Monograph Vol. 5, Henry L. Doherty Series.
- Ehlig-Economides, C. 1988. "Use of the Pressure Derivative for Diagnosing Pressure-Transient Behavior." Journal of Petroleum Technology, October 1988, pp. 1280-1282.
- Ferris, J. G., D. B. Knowles, R. H. Brown, and R. W. Stallman. 1962. Theory of Aquifer Tests, U.S. Geological Survey, Water-Supply Paper 1536-E.
- Gambolati, G. 1976. "Transient Free Surface Flow to a Well: An Analysis of Theoretical Solutions." Water Resour. Res. 12(1):27-39.
- Gilmore, T. J., J. V. Borghese, J. P. McDonald, and D. R. Newcomer. 1990. Evaluations of the Effects of the Columbia River on the Unconfined Aquifer Beneath the 1301-N Liquid Waste Disposal Facility, PNL-7341, Pacific Northwest Laboratory, Richland, Washington.
- Gilmore, T. J., F. A. Spane, Jr., D. R. Newcomer, and C. R. Sherwood. 1992. Application of Three Aquifer Test Methods for Estimating Hydraulic Properties Within the 100-N Area, PNL-8335, Pacific Northwest Laboratory, Richland, Washington.
- Hantush, M. S. 1960. "Modification of the Theory of Leaky Aquifers." J. Geophys. Res. 65(11):3713-3725.
- Hantush, M. S. 1961. "Aquifer Tests on Partially Penetrating Wells." In Proceedings of the American Society of Civil Engineers, Journal of the Hydraulics Division. (HY5):171-195.
- Hantush, M. S. 1964. "Hydraulics of Wells." In Advances in Hydroscience. Editor V. T. Chow, Vol. 1, pp. 282-433. Academic Press, New York.
- Hantush, M. S., and C. E. Jacob. 1955. "Nonsteady Radial Flow in an Infinite Leaky Aquifer." American Geophysical Union, Transactions 36(1):95-100.
- Heath, R. C. 1983. Basic Ground-Water Hydrology, U.S. Geological Survey, Water Supply Paper 2220.
- Horn, R. N. 1990. Modern Well Test Analysis: A Computer-Aided Approach. Petroway, Inc., Palo Alto, California; distributed by the Society of Petroleum Engineers. Richfield, Texas.
- Jacob, C. E. 1940. "On the Flow of Water in an Elastic Artesian Aquifer." American Geophysical Union, Transactions 14:446-460.
- Jacob, C. E. 1950. "Flow of Ground Water." In Engineering Hydraulics, H. Rouse, editor, John Wiley and Sons, Inc., New York.

Jacob, C. E. 1963. "Determining the Permeability of Water-Table Aquifers." In Bentall, R. compiler, Methods of Determining Permeability, Transmissibility, and Drawdown. U.S. Geological Survey, Water-Supply Paper 1536-I.

Karasaki, K., J.C.S. Long, and P. A. Witherspoon. 1988. "Analytical Models of Slug Tests." Water Resour. Res. 24(1):115-126.

Lennox, D. H. 1966. "Analysis and Application of Step-Drawdown Test." J. Hydraulics Division, American Society of Civil Engineers, (HY6):25-48.

Lohman, S. W. 1972. Ground-Water Hydraulics, U.S. Geological Professional Paper 708.

Mensch, A., and S. M. Benson. 1989. WES, a Robust Expert System for Well Test Analysis. Lawrence Berkeley Laboratory, LBL-27846, Berkeley, California.

Molz, F. J., O. Güven, J. G. Melville, I. Javandel, A. E. Hess, and F. L. Paillet. 1990. A New Approach and Methodologies for Characterizing the Hydrogeologic Properties of Aquifers. U.S. Environmental Protection Agency, Robert S. Kerr Environmental Research Laboratory, EPA/600/2-90/002, CR-813647, Ada, Oklahoma.

Mueller, T. D., and P. A. Witherspoon. 1965. "Pressure Interference Effects Within Reservoirs and Aquifers." Journal of Petroleum Technology, April 1965, pp. 471-474.

Neuman, S. P. 1972. "Theory of Flow in Unconfined Aquifers Considering Delayed Response of the Water Table." Water Resour. Res. 8(4):1031-1045.

Neuman, S. P. 1973. "Supplementary Comments on 'Theory of Flow in Unconfined Aquifers Considering Delayed Response of the Water Table.'" Water Resour. Res. 9(4):1102-1103.

Neuman, S. P. 1974. "Effect of Partial Penetration of Flow in Unconfined Aquifer Considering Delayed Gravity Response." Water Resour. Res. 10(2):303-312.

Neuman, S. P. 1975. "Analysis of Pumping Test Data from Anisotropic Unconfined Aquifers Considering Delayed Gravity Response." Water Resour. Res. 11(2):329-342.

Neuman, S. P. 1979. "Perspective on 'Delayed Yield.'" Water Resour. Res. 15(4):899-908.

Neuman, S. P., and P. W. Witherspoon. 1969. "Applicability of Current Theories of Flow in Leaky Aquifers." Water Resour. Res. 5(4):817-829.

Neuman, S. P., and P. W. Witherspoon. 1972. "Field Determination of the Hydraulic Properties of Leaky Multiple Systems." Water Resour. Res. 8(5):1284-1298.

- Newcomb, R. C., J. R. Strand, and F. J. Frank. 1972. Geology and Ground-Water Characteristics of the Hanford Reservation of the U.S. Atomic Energy Commission, Washington, U.S. Geological Survey, Professional Paper 717.
- Novakowski, K. S. 1990. "Analysis of Aquifer Tests Conducted in Fractured Rock: A Review of the Physical Background and the Design of a Computer Program for Generating Type Curves." Ground Water 28(1):99-105.
- Ostrowski, L. P., and M. B. Kloska. 1989. "Use of Pressure Derivatives in Analysis of Slug Test or DST Flow Period Data." Society of Petroleum Engineers, SPE paper 18595.
- Papadopoulos, I. S., and H. H. Cooper, Jr. 1967. "Drawdown in a Well of Large Diameter." Water Resour. Res. 3(1):241-244.
- Ramey, H. J., Jr. 1978. "Petroleum Engineering Well Test Analysis -- State of the Art." In Proceedings of the Invitational Well-Testing Symposium, October 19-21, 1977. Lawrence Berkeley Laboratory, LBL-7027, Berkeley, California.
- Ramey, H. J., Jr. 1982. Well-Loss Function and the Skin Effect: A Review. Geological Society of America, Special Paper 189.
- Ramey, H. J., Jr. 1992. "Advances in Practical Well-Test Analysis." Journal of Petroleum Technology, June 1992, pp. 650-659.
- Reed, J. E. 1980. Type Curves for Selected Problems of Flow to Wells in Confined Aquifers, U.S. Geological Survey, Techniques of Water-Resources Investigations, Book 3, Chapter B3.
- Rorabaugh, M. I. 1953. "Graphical and Theoretical Analysis of Step-Drawdown Tests." In Proceedings Sep. No. 362, American Society of Civil Engineers, (79).
- Spane, F. A., Jr. 1992a. Applicability of Slug Interference Tests Under Hanford Site Test Conditions: Analytical Assessment and Field Test Evaluation. PNL-8070, Pacific Northwest Laboratory, Richland, Washington.
- Spane, F. A., Jr. 1992b. Hydraulic Test Results for Savage Island Wells 699-32-22B, 699-42-E9A, and 699-42-E9B. PNL-8173, Pacific Northwest Laboratory, Richland, Washington.
- Spane, F. A., Jr., and R. B. Mercer. 1985. HEADCO: A Program For Converting Observed Water Levels and Pressure Measurements To Formation Pressure and Standard Hydraulic Head. RHO-BW-ST-71 P, Rockwell Hanford Operations, Richland, Washington.
- Spane, F. A., Jr., and S. K. Wurstner. 1992. DERIV: A Program for Calculating Pressure Derivatives For Hydrologic Test Data. PNL-SA-21569, Pacific Northwest Laboratory, Richland, Washington.

- Streltsova, T. D. 1972. "Unsteady Radial Flow in an Unconfined Aquifer." Water Resour. Res. 8(4):1059-66.
- Streltsova, T. D. 1973. "Flow Near a Pumped Well in an Unconfined Aquifer Under Nonsteady Conditions." Water Resour. Res. 9(1):227-235.
- Theis, C. V. 1935. "The Relationship Between the Lowering of the Piezometric Surface and the Rate and Duration of Discharge of a Well Using Ground-Water Storage." American Geophysical Union, Transactions, pt. 2, pp. 519-524; reprinted in Society of Petroleum Engineers, 1980 "Pressure Transient Testing Methods." SPE Reprint Series, 14:27-32.
- Thorne, P. D., and D. R. Newcomer. 1992. Summary and Evaluation of Available Hydraulic Property Data for the Hanford Site Unconfined Aquifer System. PNL-8337, Pacific Northwest Laboratory, Richland, Washington.
- Tiab, D. and A. Kumar. 1980. "Application of the p' Function to Interference Analysis." J. of Petrol. Tech., August, pp. 1465-1470.
- Walton, W. C. 1960. "Application and Limitation of Methods Used to Analyze Pumping Test Data." Water Well J., Feb.-Mar. 1960.
- Walton, W. C. 1962. Selected Analytical Methods for Well and Aquifer Evaluation. Illinois State Water Survey, Bulletin 49, Urbana, Illinois.
- Walton, W. C. 1987. Groundwater Pumping Tests. Lewis Publishers, Inc., Chelsea, Michigan.
- Weeks, E. P. 1964. Field Methods for Determining Vertical Permeability and Aquifer Anisotropy. U.S. Geological Survey, Professional Paper 501-D, pp. D193-D198.
- Weeks, E. P. 1969. "Determining the Ratio of Horizontal to Vertical Permeability by Aquifer-Test Analysis." Water Resour. Res. 5(1):196-214.
- Weeks, E. P. 1978. "Aquifer Tests -- The State of the Art in Hydrology." In Proceedings of the Invitational Well-Testing Symposium, October 19-21, 1977. Lawrence Berkeley Laboratory, LBL-7027, Berkeley, California.
- Weeks, E. P. 1979. "Barometric Fluctuations in Wells Tapping Deep Unconfined Aquifers." Water Resour. Res. 15(5):1167-1176.
- Witherspoon, P. A. 1978. "Well Testing, A Recapitulation of Its Development." In Proceedings of the Invitational Well-Testing Symposium, October 19-21, 1977. Lawrence Berkeley Laboratory, LBL-7027, Berkeley, California.

DISTRIBUTION

<u>No. of Copies</u>		<u>No. of Copies</u>	
	<u>OFFSITE</u>	49	<u>Pacific Northwest Laboratory</u>
2	DOE/Office of Scientific and Technical Information		J. V. Borghese R. W. Bryce C. R. Cole J. L. Devary P. G. Doctor M. D. Freshley T. J. Gilmore R. H. Gray R. E. Jaquish G. V. Last T. L. Liikala P. E. Long S. P. Luttrell D. R. Newcomer S. A. Rawson R. Schalla R. E. Schrempf F. A. Spane (20) P. D. Thorne V. R. Vermeul W. D. Webber R. E. Wildung S. K. Wurstner Publishing Coordination Technical Report Files (5)
	<u>ONSITE</u>		
9	<u>DOE Richland Field Office</u>		
	M. J. Furman E. D. Goller A. C. Harris R. D. Hildebrand R. G. McLeod P. Pak R. K. Stewart K. M. Thompson M. W. Tiernan		
12	<u>Westinghouse Hanford Company</u>		
	C. D. Delaney K. R. Fecht M. J. Hartman R. L. Jackson A. J. Knepp A. G. Law W. J. McMahon R. E. Peterson L. C. Swanson S. J. Trent D. K. Tyler S. E. Vukelich		
2	<u>U.S. Army Corps of Engineers</u>		
	J. T. Stewart W. Greenwald		
			<u>Routing</u>
			R. M. Ecker M. J. Graham C. J. Hostetler P. M. Irving R. L. Skaggs C. S. Sloane P. C. Hays (last)

**DATE
FILMED**

7 / 12 / 93

